

Novel Ruthenium(II) Carbene Complexes: Products of the Reactions of 1-Alkynes with $(\eta^6\text{-C}_6\text{Me}_6)\text{Cl}_2\text{Ru}(\text{PR}_3)$

Heather D. Hansen and John H. Nelson*

Department of Chemistry/216, University of Nevada—Reno, Reno, Nevada 89557-0020

Received June 13, 2000

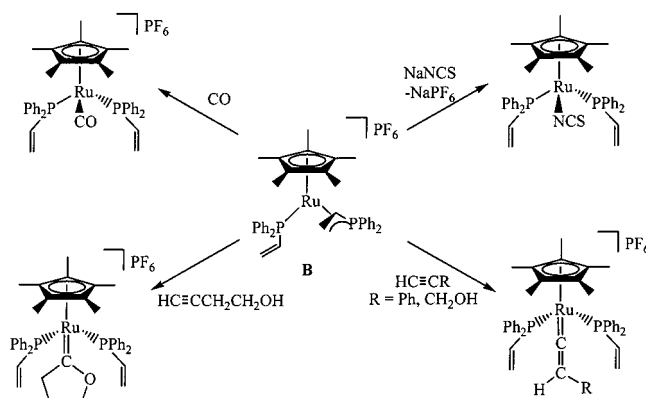
The complexes $(\eta^6\text{-C}_6\text{Me}_6)\text{Cl}_2\text{Ru}(\text{PR}_3)$ (**1**; $\text{PR}_3 = \text{DPVP}$ (diphenylvinylphosphine) (**a**), PMe_3 (**b**), PPh_3 (**c**)) react with NaPF_6 in acetonitrile solutions to give the cationic complexes $[(\eta^6\text{-C}_6\text{Me}_6)\text{ClRu}(\text{PR}_3)(\text{NCCCH}_3)]\text{PF}_6$ (**2a–c**) by loss of NaCl . Complexes **1a** and **2a** react with $\text{HC}\equiv\text{CSiMe}_3$ and $\text{HC}\equiv\text{CPh}$ (and NaPF_6 for **1a**) in MeOH to give the carbene complexes $[(\eta^6\text{-C}_6\text{Me}_6)\text{Cl}(\text{DPVP})\text{Ru}=\text{C}(\text{OCH}_3)\text{CH}_3]\text{PF}_6$ (**3a**) and $[(\eta^6\text{-C}_6\text{Me}_6)\text{Cl}(\text{DPVP})\text{Ru}=\text{C}(\text{OCH}_3)\text{CH}_2\text{Ph}]\text{PF}_6$ (**4a**), respectively. The known analogues **3b,c** and **4b** and the new complex **4c** have been synthesized from **2b,c** and $\text{HC}\equiv\text{CR}$. The solid-state structures of these complexes show a wide variation in the orientation of the carbene plane with respect to the plane of the η^6 -arene ring (dihedral angles of $37.9\text{--}59.6^\circ$). The solution dynamic behavior of **3a–c** and **4a–c** is discussed. Complex **2a** also reacts with $\text{HC}\equiv\text{CCH}_2\text{CH}_2\text{OH}$ in MeOH to give the oxacyclic carbene complex $[(\eta^6\text{-C}_6\text{Me}_6)\text{Cl}(\text{DPVP})\text{Ru}=\text{C}(\text{CH}_2\text{CH}_2\text{CH}_2\text{O})]\text{PF}_6$ (**5**). **1a** (and NaPF_6) and **2a** react with $\text{HC}\equiv\text{CC}(\text{OH})\text{Ph}_2$ in MeOH to give the novel phosphorus ylide complex $[(\eta^6\text{-C}_6\text{Me}_6)\text{ClRu}(\text{C}=\text{C}(\text{Ph}_2)\text{PPh}_2\text{CH}=\text{CH}_2)]\text{PF}_6$ (**6**) and with dimethylpropargylamine in CH_2Cl_2 or dichloroethane to give the amino cyclic carbene complex $[(\eta^6\text{-C}_6\text{Me}_6)\text{Cl}(\text{DPVP})\text{Ru}=\text{CCH}_2\text{CMe}_2\text{NH}]\text{PF}_6$ (**7**) and the metallacyclic complex $[(\eta^6\text{-C}_6\text{Me}_6)\text{ClRuCH}=\text{C}(\text{DPVP})\text{CMe}_2\text{NH}_2]\text{PF}_6$ (**8**). In the absence of MeOH , reaction of **2a** with $\text{HC}\equiv\text{CC}(\text{OH})\text{Ph}_2$ gives the dimeric complex $[(\eta^6\text{-C}_6\text{Me}_6)\text{Ru}(\mu\text{-Cl})_3\text{Ru}(\eta^6\text{-C}_6\text{Me}_6)]\text{PF}_6$. Complex **2a** plus $\text{HC}\equiv\text{CPh}$ in the absence of MeOH gives the carbonyl complex $[(\eta^6\text{-C}_6\text{Me}_6)\text{Cl}(\text{DPVP})\text{Ru}(\text{CO})]\text{PF}_6$ (**9**). Reaction of **2c** with $\text{HC}\equiv\text{CPh}$ in MeOH for extended time periods (>1 day) gives an analogous carbonyl complex of PPh_3 , $[(\eta^6\text{-C}_6\text{Me}_6)\text{Cl}(\text{PPh}_3)\text{Ru}(\text{CO})]\text{PF}_6$. All complexes have been characterized by ^1H , $^{13}\text{C}\{^1\text{H}\}$, and $^{31}\text{P}\{^1\text{H}\}$ NMR and IR spectroscopies and electrochemistry and in most cases by X-ray crystallography. Complex **1a** is an efficient catalyst for the regioselective addition of H_2O to $\text{HC}\equiv\text{CPh}$, producing exclusively acetophenone in 70% isolated yield.

Introduction

Previous investigations in our laboratory with the hybrid hemilabile ligand diphenylvinylphosphine (DPVP) resulted in the synthesis of the phosphaaallyl complexes $[(\eta^5\text{-C}_5\text{H}_5)\text{Ru}(\eta^3\text{-DPVP})(\eta^1\text{-DPVP})]\text{PF}_6$ (**A**)¹ and $[(\eta^5\text{-C}_5\text{Me}_5)\text{Ru}(\eta^3\text{-DPVP})(\eta^1\text{-DPVP})]\text{PF}_6$ (**B**).² The η^3 -DPVP ligand is a neutral, monometallic phosphaaallyl ligand coordinated to ruthenium through its phosphorus atom and its vinyl group. The hemilabile nature of the η^3 -DPVP ligand in complex **B** was demonstrated by the reactions illustrated in Scheme 1. Similar reactions showed the hemilabile nature of the phosphaaallyl ligand in complex **A**.¹

As an extension of the chemistry of ruthenium–DPVP complexes and of the chemistry of $(\eta^6\text{-arene})\text{ruthenium}$ complexes, we attempted to synthesize $[(\eta^6\text{-C}_6\text{Me}_6)\text{ClRu}(\eta^3\text{-DPVP})]\text{PF}_6$ (**C**). Though we have been unable to confirm the formation of **C**, its acetonitrile precursor $[(\eta^6\text{-C}_6\text{Me}_6)\text{ClRu}(\eta^1\text{-DPVP})(\text{NCCCH}_3)]\text{PF}_6$ reacts with

Scheme 1. Reactions of the Phosphaaallyl Complex B



terminal alkynes to form traditional and novel carbene complexes.

We report here (1) the synthesis and characterization of two new $\eta^6\text{-C}_6\text{Me}_6$ –phosphine–ruthenium–acetonitrile

(1) Ji, H.-L.; Nelson, J. H.; DeCian, A.; Fischer, J.; Solujić, L.; Milosavljević, E. B. *Organometallics* **1992**, *11*, 401.

(2) Barthel-Rosa, L. P.; Maitra, K.; Fischer, J.; Nelson, J. H. *Organometallics* **1997**, *16*, 1714.

(3) Redwine, K. D.; Hansen, H. D.; Bowley, S.; Isbell, J.; Vodak, D.; Nelson, J. H. *Synth. React. Inorg. Met.-Org. Chem.* **2000**, *30*, 409.

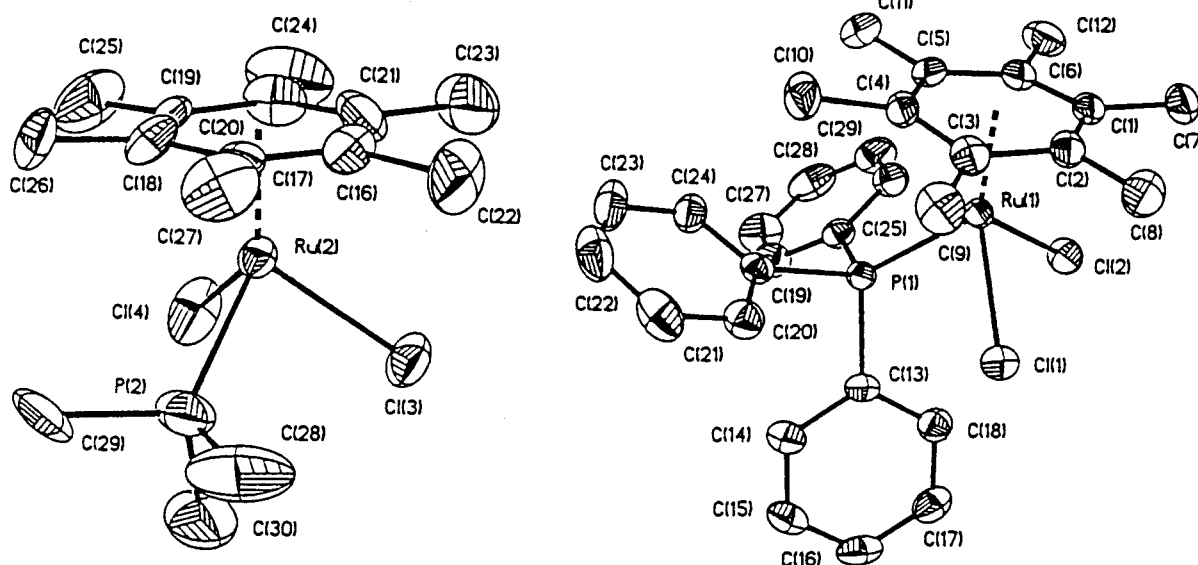


Figure 1. Structural drawings of $(\eta^6\text{-C}_6\text{Me}_6)\text{Cl}_2\text{Ru}(\text{PMe}_3)$ (**1b**) and $(\eta^6\text{-C}_6\text{Me}_6)\text{Cl}_2\text{Ru}(\text{PPh}_3)$ (**1c**) showing the atom-numbering schemes (30% probability ellipsoids). Hydrogen atoms have been omitted for clarity.

trile complexes and their reactions with terminal alkynes, (2) structural characterization of a series of $\eta^6\text{-C}_6\text{Me}_6$ -phosphine-ruthenium-carbene complexes, (3) complete analysis of the dynamic behavior of these carbene complexes by ^1H , $^{13}\text{C}\{^1\text{H}\}$, and $^{31}\text{P}\{^1\text{H}\}$ variable-temperature NMR spectroscopy and NOE experiments, (4) four new complexes (including two new complex types) containing the $[(\eta^6\text{-C}_6\text{Me}_6)\text{ClRu}(\text{DPVP})]$ moiety, and (5) the use of $(\eta^6\text{-C}_6\text{Me}_6)\text{Cl}_2\text{Ru}(\text{DPVP})$ to catalyze the hydration of phenylacetylene.

Results and Discussion

Structural Characterization of $(\eta^6\text{-C}_6\text{Me}_6)\text{Cl}_2\text{Ru}(\text{PR}_3)$ (1**).** Bridge cleavage of the dimeric $[(\eta^6\text{-C}_6\text{Me}_6)\text{-RuCl}_2]_2$ complex with 2 equiv of a phosphine gives the reported complexes $(\eta^6\text{-C}_6\text{Me}_6)\text{Cl}_2\text{Ru}(\text{PR}_3)$ (**1**; PR_3 = diphenylvinylphosphine (DPVP) (**a**),⁴ PMe_3 (**b**),⁵ PPh_3 (**c**)⁶). The physical properties and NMR and IR spectral data for **1a–c** have been reported.^{4–6} The molecular structures of **1b,c** were determined, and views of their crystal structures are given in Figure 1. Selected bond distances and angles are given in Table 1. The structures of **1b,c** consist of isolated molecules with no unusual intermolecular contacts, and their metrical parameters compare favorably with those of similar three-legged piano-stool $(\eta^6\text{-arene})\text{Cl}_2\text{Ru}(\text{PR}_3)$ complexes in which the Ru(II) atoms possess a pseudo-octahedral geometry.^{4,7}

Synthesis and Characterization of $[(\eta^6\text{-C}_6\text{Me}_6)\text{-Cl}(\text{PR}_3)\text{Ru}(\text{NCCH}_3)]\text{PF}_6$ (2**).** Reaction of **1a–c** with 1 equiv of NaPF_6 in acetonitrile/ CH_2Cl_2 solutions readily gave the cationic complexes $[(\eta^6\text{-C}_6\text{Me}_6)\text{Cl}(\text{PR}_3)\text{Ru}(\text{NCCH}_3)]\text{PF}_6$ (**2a–c**) and NaCl , as was reported for **2a**.³ Removal of NaCl followed by crystallization gave an 87%

Table 1. Selected Bond Distances (Å) and Angles (deg) for $(\eta^6\text{-C}_6\text{Me}_6)\text{Cl}_2\text{Ru}(\text{PR}_3)$ (**1b,c**)

	$(\eta^6\text{-C}_6\text{Me}_6)\text{Cl}_2\text{Ru}(\text{PMe}_3)$ (1b)	$(\eta^6\text{-C}_6\text{Me}_6)\text{Cl}_2\text{Ru}(\text{PPh}_3)$ (1c)
Ru–P	2.343(3)	2.3607(10)
Ru–Cl(1)	2.422(3)	2.4117(10)
Ru–Cl(2)	2.424(3)	2.4118(10)
Ru–C(ave.)	2.215(11)	2.249(4)
P–Ru–Cl(1)	82.4(11)	84.99(3)
P–Ru–Cl(2)	84.96(11)	88.22(4)
Cl(1)–Ru–Cl(2)	90.31(10)	88.16(4)
$\Sigma \angle^a$	257.31	261.37

^a $\Sigma \angle$ = the sum of the P–Ru–Cl(1), P–Ru–Cl(2), and Cl(1)–Ru–Cl(2) angles.

yield of **2b** and a 28% yield of **2c** as orange-yellow powders. Complex **2c** was contaminated with the triply chloride bridged dimer $[(\eta^6\text{-C}_6\text{Me}_6)\text{Ru}(\mu\text{-Cl})_3\text{Ru}(\eta^6\text{-C}_6\text{Me}_6)]\text{PF}_6$,⁴ which was removed by repeated recrystallizations from $\text{CH}_2\text{Cl}_2/\text{Et}_2\text{O}$.

Complex **2b** is quite soluble in acetone, CH_3OH , and CH_3NO_2 , less soluble in CH_2Cl_2 and CHCl_3 , and not soluble in ether and hydrocarbons. Complex **2c** follows the same trend, but it is less soluble than **2b** in all solvents. Complexes **2b,c** are not stable for extended periods in any solvent. Complexes **2b,c** were identified by the appearance of $\nu(\text{C}\equiv\text{N})$ stretching vibrations (at 2322 and 2328 cm^{-1} , respectively) in their infrared spectra and the resonances for coordinated CH_3CN in their ^1H and $^{13}\text{C}\{^1\text{H}\}$ NMR spectra (see Experimental Section). Also characteristic of the formation of cationic species, their $^{31}\text{P}\{^1\text{H}\}$ NMR resonances are shifted downfield relative to those of **1b,c**. Similar observations have been made for the transformation of $(\eta^6\text{-arene})\text{-RuCl}_2(\text{PR}_3)$ ⁴ to $[(\eta^6\text{-arene})\text{RuCl}(\text{PR}_3)(\text{NCCH}_3)]\text{PF}_6$ ³ for several arene and PR_3 combinations.

The Ru(II)/Ru(III) redox potentials of complexes **1a–c** have been reported to be 0.47,⁴ 0.32,⁸ and 0.47 V,⁸ respectively. This shows the PMe_3 complex to be more easily oxidized because of the greater σ -donor ability of

(4) Redwine, K. D.; Hansen, H. D.; Bowley, S.; Isbell, J.; Sanchez, M.; Vodak, D.; Nelson, J. H. *Synth. React. Inorg. Met.-Org. Chem.* **2000**, *30*, 379.

(5) Werner, H.; Werner, R. *Chem. Ber.* **1982**, *115*, 3766.

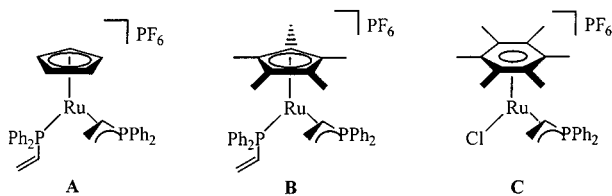
(6) Bennett, M. A.; Huang, T.-N.; Latten, J. L. *J. Organomet. Chem.* **1984**, *272*, 189.

(7) Bennett, M. A.; Robertson, G. B.; Smith, A. K. *J. Organomet. Chem.* **1972**, *43*, C41.

(8) Štěpnička, P.; Gyepes, R.; Lavastre, O.; Dixneuf, P. H. *Organometallics* **1997**, *16*, 5089.

PMe_3 , and it indicates very similar σ -donor abilities of PPh_3 and DPVP. For complexes **2a–c**, the redox couples are more positive, as expected for cationic species. The redox couple for **2a** was reported to be 0.96 V,³ and the redox couple of **2b** was found to be 1.03 V, an unexpected trend. Complex **2c** shows only an oxidation wave (1.21 V) and several electrochemical events at negative potentials, indicating redox instability of this complex. As will be shown later, reactions with **2c** result in large amounts of decomposition in all solvents and under all conditions utilized; therefore, its decomposition under electrochemical stress is not unexpected.

We initially prepared **2a** because of our desire to prepare $[(\eta^6\text{-C}_6\text{Me}_6)\text{ClRu}(\eta^3\text{-DPVP})]\text{PF}_6$ (**C**), which contains the hybrid hemilabile phosphaa allyl ligand η^3 -DPVP.



Complex **C** would be the arene analogue of the novel Cp and Cp* complexes **A** and **B**, prepared previously in our laboratories,^{1,2} from the corresponding $[(\text{Cp}/\text{Cp}^*)\text{-Ru}(\eta^1\text{-DPVP})_2(\text{NCCH}_3)]\text{PF}_6$ complexes by removal of CH_3CN in vacuo. Both in solution and in the solid state **A** and **B** contain the η^3 -phosphaa allyl ligand, which is stabilized by π -electron donation from Ru to the $\text{CH}=\text{CH}_2$ group. The vinyl moiety in **A** and **B** is easily displaced by a variety of two-electron-donor ligands (Scheme 1). As would be expected on the basis of the greater electron-donating ability of C_5Me_5 vs C_5H_5 , **B** is more easily formed than **A** from the corresponding $[(\text{Cp}/\text{Cp}^*)\text{Ru}(\eta^1\text{-DPVP})_2(\text{NCCH}_3)]\text{PF}_6$ species.² Since both Cp* and Cp are better electron-donating ligands than $\eta^6\text{-C}_6\text{Me}_6$, we expected that **C** might be difficult to obtain from its corresponding acetonitrile complex **2a**. Heating **2a** at 112 °C for 2 weeks under reduced pressure gave a complex mixture, as seen by ^1H and $^{31}\text{P}\{^1\text{H}\}$ NMR spectroscopy, from which we have been able to isolate neither **C** nor **2a**. Nonetheless, **2a** is a cationic species with a very labile CH_3CN ligand that is readily replaced by alkynes. Use of **2a** eliminates the need for reaction with NaPF_6 and subsequent removal of NaCl , since this step has already been accomplished in the preparation of **2a** from **1a**. Reaction of **2a** with alkynes proceeded cleanly and with high yields (78–90%); therefore, we have employed it and complexes **2b,c** in our studies.

Synthesis, Characterization, and X-ray Crystal Structures of Methoxyalkylcarbenes $[(\eta^6\text{-C}_6\text{Me}_6)\text{-Cl}(\text{PR}_3)\text{Ru}=\text{C}(\text{OCH}_3)\text{CH}_2\text{R}']\text{PF}_6$ ($\text{R}' = \text{H}$ (3**), Ph (**4**)).** Reaction of **2a–c** with $\text{HC}\equiv\text{CSiMe}_3$ and $\text{HC}\equiv\text{CPh}$ gave the methoxymethylcarbene complexes $[(\eta^6\text{-C}_6\text{Me}_6)\text{Cl}(\text{PR}_3)\text{Ru}=\text{C}(\text{OCH}_3)\text{CH}_3]\text{PF}_6$ (**3a–c**) and the methoxybenzylcarbene complexes $[(\eta^6\text{-C}_6\text{Me}_6)\text{Cl}(\text{PR}_3)\text{Ru}=\text{C}(\text{OCH}_3)\text{CH}_2\text{Ph}]\text{PF}_6$ (**4a–c**), respectively, as shown in Scheme 2. The formation of complexes **3b** and **4b,c** was confirmed by comparison of their NMR spectral data with those reported by Dixneuf and co-workers.⁹ The new complexes **3a,c** and **4a** were also characterized by

Scheme 2. Synthesis of Methoxyalkylcarbene Complexes **3** and **4**

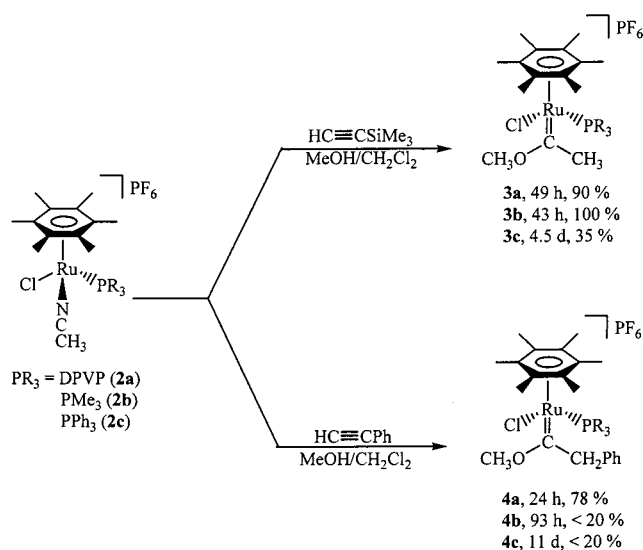


Table 2. Selected $^{13}\text{C}\{^1\text{H}\}$, ^1H , and $^{31}\text{P}\{^1\text{H}\}$ NMR Spectral Data for the Methoxyalkylcarbene Complexes $[(\eta^6\text{-C}_6\text{Me}_6)\text{Cl}(\text{PR}_3)\text{Ru}=\text{C}(\text{OCH}_3)\text{CH}_3]^+$ (3**) and $[(\eta^6\text{-C}_6\text{Me}_6)\text{Cl}(\text{PR}_3)\text{Ru}=\text{C}(\text{OCH}_3)\text{CH}_2\text{Ph}]^+$ (**4**), in ppm (J in Hz)**

PR_3	$\delta(^{13}\text{C})$ Ru=C	$\delta(^1\text{H})$			$\delta(^{31}\text{P})$ PR_3
		OCH_3	CH_3	CH_2	
DPVP (3a)	327.99 (19.9)	4.38	2.87		31.31
PMe_3^a (3b)	330.86 (21.2)	4.48	2.98		10.50
PPh_3 (3c)	331.00 (19.6)	4.18	2.91		38.14
DPVP (4a)	314.54 (14.5)	4.50		5.07, 3.23 (12.5)	27.95
PMe_3^a (4b)	323.10 (20.64)	4.59		5.04, 4.50 (13.0)	8.12
PPh_3^a (4c)	316.60 (18.65)	4.50		4.76, 2.65 (13.03)	36.06

^a Reference 9a.

NMR spectroscopy. Diagnostic $^{13}\text{C}\{^1\text{H}\}$, ^1H , and $^{31}\text{P}\{^1\text{H}\}$ NMR data for the six carbene complexes are compared in Table 2. The carbene carbon chemical shifts all occur between 310 and 335 ppm with two-bond P–C coupling constants on the order of 18–20 Hz. The ^1H NMR spectral data of the carbene ligands vary only slightly. The vinyl protons of the DPVP group in **3a** and **4a** show the characteristic^{1–4} set of multiplets between 6.9 and 5.3 ppm (see Experimental Section).

Complexes **3a–c** and **4a–c** were characterized by X-ray crystallography. Views of the structures of the cations are shown in Figure 2; selected bond distances are given in Table 3, and selected bond angles are given in Table 4. The bond lengths and angles are similar among the cations of each molecule. Analysis of all six structures shows a distorted-octahedral geometry about Ru with the $\eta^6\text{-C}_6\text{Me}_6$ ligand occupying three facial coordination sites and the three remaining ligands (Cl, PR_3 , and carbene) completing the coordination sphere. The Ru=C(carbene) bond lengths of 1.94–2.02 Å are similar to those reported for other structurally characterized Ru carbene complexes.^{8,9d,10} The dihedral angles vary considerably among the complexes (37.9–59.6°),

(9) (a) Le Bozec, H.; Ouzzine, K.; Dixneuf, P. H. *Organometallics* **1991**, *10*, 2768. (b) Ouzzine, K.; Le Bozec, H.; Dixneuf, P. H. *J. Organomet. Chem.* **1986**, *317*, C25. (c) Dixneuf, P. H. *Pure Appl. Chem.* **1989**, *61*, 1763. (d) Pilette, D.; Ouzzine, K.; Le Bozec, H.; Dixneuf, P. H.; Rickard, C. E. F.; Roper, W. R. *Organometallics* **1992**, *11*, 809.

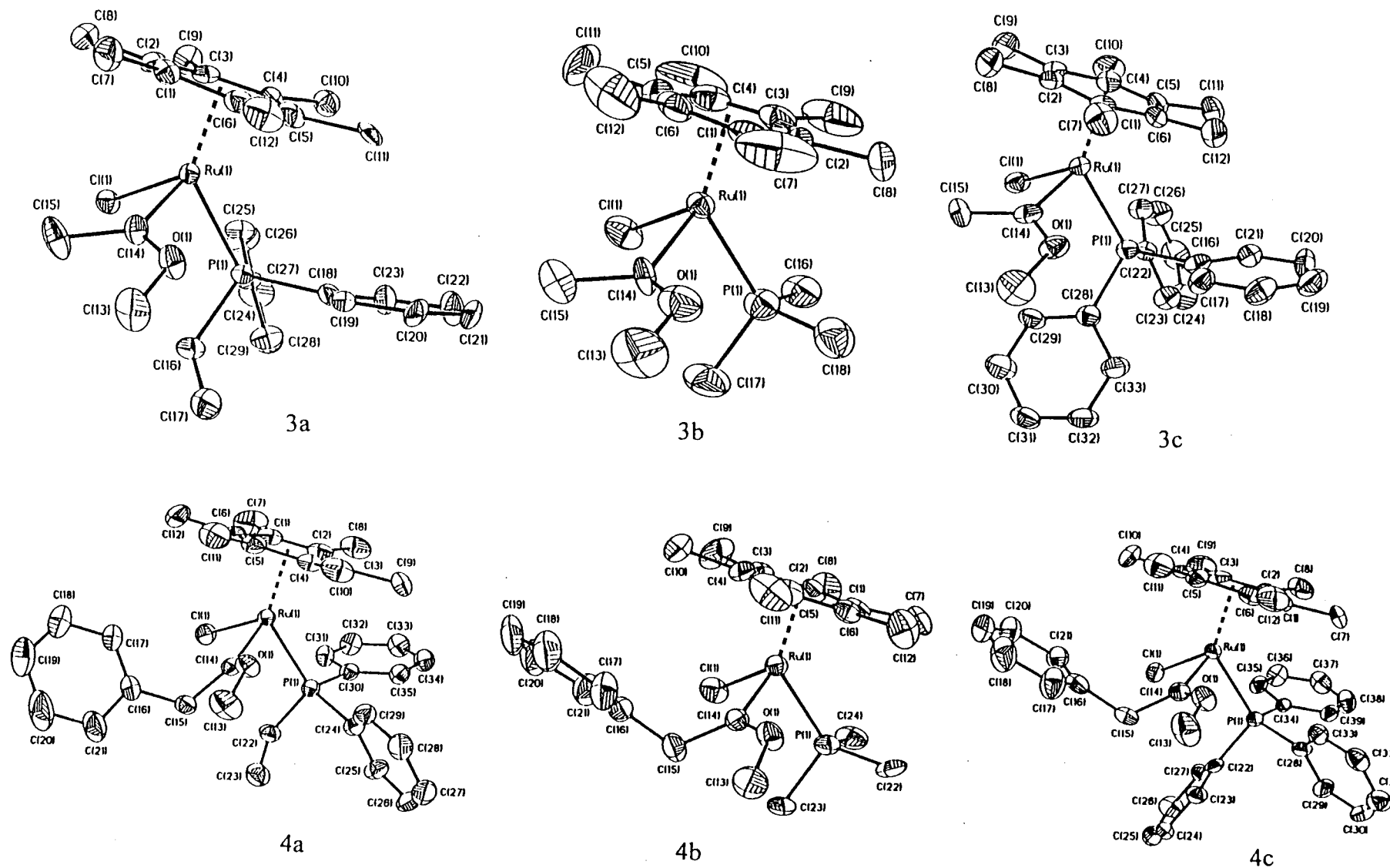


Figure 2. Structural drawings of the cations of $[(\eta^6\text{-C}_6\text{Me}_6)\text{Cl}(\text{PR}_3)\text{Ru}=\text{C}(\text{OCH}_3)\text{CH}_3]\text{PF}_6$ ($\text{PR}_3 = \text{DPVP}$ (**3a**), PMe_3 (**3b**), PPh_3 (**3c**)) and $[(\eta^6\text{-C}_6\text{Me}_6)\text{Cl}(\text{PR}_3)\text{Ru}=\text{C}(\text{OCH}_3)\text{-CH}_2\text{Ph}]\text{PF}_6$ ($\text{PR}_3 = \text{DPVP}$ (**4a**), PMe_3 (**4b**), PPh_3 (**4c**)) showing the atom-numbering schemes (30% probability ellipsoids). Hydrogen atoms have been omitted for clarity.

Table 3. Selected Bond Distances (Å) for Methoxyalkylcarbene Compounds $[(\eta^6\text{-C}_6\text{Me}_6)\text{Cl}(\text{PR}_3)\text{Ru}=\text{C}(\text{OCH}_3)\text{CH}_2\text{R}']\text{PF}_6$ (3a–c and 4a–c)

	Ru–C(14)	Ru–P	Ru–Cl	Ru–C (av)	C(14)–C(15)	C(14)–O
3a	1.964(10)	2.342(3)	2.400(3)	2.295(13)	1.497(16)	1.309(12)
3b	2.015(8)	2.311(3)	2.403(3)	2.278(11)	1.523(14)	1.256(11)
3c	1.962(10)	2.351(3)	2.400(3)	2.320(11)	1.490(14)	1.300(12)
4a	1.956(7)	2.3364(18)	2.3993(18)	2.334(7)	1.515(9)	1.328(8)
4b	1.955(13)	2.327(4)	2.407(3)	2.303(14)	1.508(17)	1.306(14)
4c	1.939(10)	2.354(2)	2.404(3)	2.322(10)	1.529(13)	1.288(10)

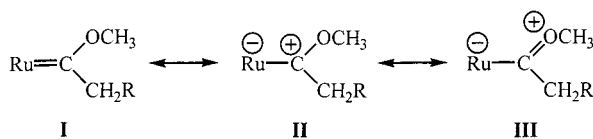
Table 4. Selected Bond Angles (deg) for Methoxyalkylcarbene Compounds $[(\eta^6\text{-C}_6\text{Me}_6)\text{Cl}(\text{PR}_3)\text{Ru}=\text{C}(\text{OCH}_3)\text{CH}_2\text{R}']\text{PF}_6$ (3a–c and 4a–c)

	P–Ru–C(14)	Cl–Ru–C(14)	P–Ru–Cl	Ru–C(14)–C(15)	Ru–C(14)–O	O–C(14)–C(15)	dihedral angle ^a
3a	86.6(3)	89.1(3)	85.19(11)	124.5(8)	118.5(8)	117.0(9)	79.9
3b	81.9(3)	89.8(3)	85.55(12)	121.6(8)	116.7(6)	118.5(9)	78.1
3c	86.2(3)	90.8(3)	88.75(10)	124.3(8)	118.3(8)	117.2(10)	92.3
4a	86.09(19)	91.7(2)	87.06(7)	127.6(5)	115.7(5)	116.7(6)	37.9
4b	82.5(4)	93.0(4)	84.44(14)	126.8(10)	115.5(9)	117.6(12)	59.6
4c	88.8(3)	91.7(3)	84.32(9)	127.3(8)	115.8(7)	116.8(9)	57.7

^a Defined as the angle between the C(arene centroid)–Ru–C(carbene) and CH_2R –C(carbene)– OCH_3 planes.

where the dihedral angle is defined as the angle between the C(arene centroid)–Ru–C(carbene) and CH_2R –C(carbene)– OCH_3 planes. This difference in observed dihedral angles led us to study the dynamic behavior of these complexes by variable-temperature NMR spectroscopy.

Dynamic Behavior of the Methoxyalkylcarbene Complexes $[(\eta^6\text{-C}_6\text{Me}_6)\text{Cl}(\text{PR}_3)\text{Ru}=\text{C}(\text{OCH}_3)\text{CH}_2\text{R}']\text{PF}_6$ (3a–c, 4a–c). Three canonical representations can be drawn for these Fischer-type carbene complexes (**I**–**III**).^{10a,11} These representations differ in the localization



of electron density in the three-atom π system (Ru–C–O). If we consider a carbene to be a neutral two-electron-donor ligand, the other two electrons in the $\text{Ru}=\text{C}$ double bond must come from the metal. Hence, greater electron density on the metal (low oxidation state and/or electron-donating substituents) favors form **I** and a rigid metal–carbon bond about which little to no rotation is anticipated. As the electron-donating ability of the metal decreases, forms **II** and **III** become more important. In the limit of no contribution from **I**, forms **II** and **III** suggest free rotation about a Ru–C single bond. Complexes with contributions from all three forms are then expected to show hindered rotation about the ruthenium–carbon bond, the magnitude of the barrier being dependent upon the amount of $\text{Ru}_{d\pi} \rightarrow \text{C}_{p\pi}$ back-donation.

Theoretical studies of the bonding in late-transition-metal carbene complexes predict barriers to rotation about the $\text{M}=\text{C}$ double bond on the order of 6–12 kcal/

mol.¹² VT NMR spectroscopic studies agree with the theoretical predictions.¹³ Theoretical and variable-temperature NMR spectroscopic studies of ruthenium–vinylidene complexes show the barrier to rotation about the Ru–C bond to be 9–10 kcal/mol.¹⁴ Theoretical studies predict the lower energy conformations to be that with a “vertical” carbene for cyclopentadienyl (CpML_2) complexes and that with a “horizontal” carbene for (arene) ML_2 complexes. For most of the reported structurally characterized CpML_2 carbenes, the vertical orientation is found. For the three reported structurally characterized (arene) ML_2 carbenes ($[(\eta^6\text{-C}_6\text{Me}_6)\text{Ru}(\text{C}(\text{OCH}_3)\text{CH}_2\text{Fc})\{(\eta^5\text{-C}_5\text{H}_4\text{PPh}_2)\text{Fe}(\eta^5\text{-C}_5\text{H}_4\text{COOH})\}\text{P}\}(\text{Cl})]\text{PF}_6$ (Fc = ferrocenyl),⁸ $[(\eta^6\text{-C}_6\text{Me}_6)(\text{PMe}_3)\text{ClRu}=\text{C}(\text{OCH}_3)\text{CH}=\text{CPh}_2]\text{PF}_6$,^{9d} and $(\eta^6\text{-C}_6\text{H}_6)(\text{CO})_2\text{Cr}=\text{C}(\text{OEt})\text{-Ph}^{15}$) a horizontal orientation was found. These differences have been interpreted on the basis of both electronic (maximum attractive π overlap and minimizing orbital energies) and steric influences.

For the methoxyalkylcarbenes described here, the dihedral angles vary from 37.9 to 59.6°, indicating interplay of electronic and steric influences in the solid state. We have attempted no molecular orbital calculations to discern the complete nature of the electronic influences on the solid-state structures. We have determined the rotational barriers for this series of complexes to gain knowledge of the degree of Ru–C double vs single bond character, i.e. canonical form **I** vs forms **II** and **III**. ¹H NOE experiments showed all six complexes to be dynamic at room temperature. Variable-temperature ¹H, ³¹P{¹H}, and ¹³C{¹H} NMR spectra were recorded for acetone-*d*₆ solutions of each of the complexes (**3a–c** and **4a–c**) between +50 and –90 °C. The

(10) (a) Schubert, U. In *Transition Metal Carbene Complexes*; Verlag Chemie: Weinheim, Germany, 1983; p 113. (b) Bianchini, C.; Masì, D.; Romerosa, A.; Zanolini, F.; Peruzzini, M. *Organometallics* **1999**, *18*, 2376. (c) Stockman, K. E.; Sabat, M.; Finn, M. G.; Grimes, R. N. *J. Am. Chem. Soc.* **1992**, *114*, 8733. (d) Consiglio, G.; Morandini, F.; Ciani, G. F.; Sironi, A. *Organometallics* **1986**, *5*, 1976.

(11) (a) Collman, J. P.; Hegedus, L. S.; Norton, J. R.; Finke, R. G. *Principles and Applications of Organotransition Metal Chemistry*; University Science Books: Mill Valley, CA, 1987; pp 119–136. (b) Schubert, U. *Coord. Chem. Rev.* **1984**, *55*, 261.

(12) (a) Schilling, B. E. R.; Hoffmann, R.; Lichtenberger, D. L. *J. Am. Chem. Soc.* **1979**, *101*, 585. (b) Kostić, N. M.; Fenske, R. F. *Organometallics* **1982**, *1*, 974. (c) Kostić, N. M.; Fenske, R. F. *J. Am. Chem. Soc.* **1982**, *104*, 3879. (d) Hofmann, P. In *Transition Metal Carbene Complexes*; Verlag Chemie: Weinheim, Germany, 1983; p 73.

(13) (a) Brookhart, M.; Tucker, J. R.; Flood, T. C.; Jensen, J. *J. Am. Chem. Soc.* **1980**, *102*, 1203. (b) Studabaker, W. B.; Brookhart, M. *J. Organomet. Chem.* **1986**, *310*, C39. (c) Kegley, S. E.; Brookhart, M.; Husk, G. R. *Organometallics* **1982**, *1*, 760. (d) Brumaghim, J. L.; Girolami, G. S. *Chem. Commun.* **1999**, 953. (e) Guerchais, V.; Lapinte, C.; Thépot, J.-Y.; Toupet, L. *Organometallics* **1988**, *7*, 604.

(14) (a) Consiglio, G.; Morandini, F. *Inorg. Chim. Acta* **1987**, *127*, 79. (b) Urtel, K.; Frick, A.; Huttner, G.; Zsolnai, L.; Kircher, P.; Rutsch, P.; Kaifer, E.; Jacobi, A. *Eur. J. Inorg. Chem.* **2000**, 33.

(15) Schubert, U. *J. Organomet. Chem.* **1980**, *185*, 373.

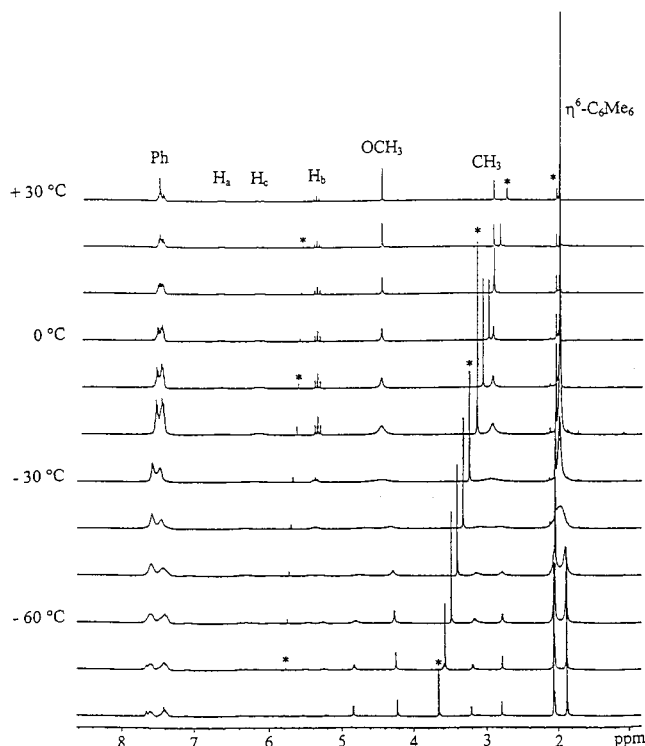


Figure 3. Variable-temperature ^1H NMR spectra of $[(\eta^6\text{-C}_6\text{Me}_6)\text{Cl}(\text{DPVP})\text{Ru}=\text{C}(\text{OCH}_3)\text{CH}_3]\text{PF}_6$ (**3a**) from $+30\text{ }^\circ\text{C}$ to $-80\text{ }^\circ\text{C}$ in acetone- d_6 , clearly showing splitting of the CH_3 , OCH_3 , and $\eta^6\text{-C}_6\text{Me}_6$ resonances with decreasing temperature. The resonances marked with an asterisk (*) are due to solvents.

PMe_3 complexes **3b** and **4b** showed very little change (and no splitting of resonances) upon lowering the temperature in their ^1H and $^{31}\text{P}\{^1\text{H}\}$ NMR spectra; we conclude that the carbene ligand is freely rotating about the $\text{Ru}-\text{C}$ bond at all temperatures above $-90\text{ }^\circ\text{C}$. Electronically, this indicates a very low or negligible barrier to rotation and a large contribution from canonical form **II** and/or **III**. Sterically, this result could be anticipated because of the relatively small size of the PMe_3 ligand.

Complexes **3a,c** and **4a,c** show a very interesting phenomenon. The ^1H VT NMR spectral data for complex **3a** are shown in Figure 3; the corresponding Eyring plot is given in Figure 4. The Eyring plot clearly shows the presence of two separate, though probably interrelated, dynamic processes. The activation enthalpy and entropy for the dominant process at lower temperature are 2.3 kcal/mol and -35.4 cal/(mol K) , respectively, which gives $\Delta G^\ddagger_{298} = 12.8\text{ kcal/mol}$. The corresponding values for the process dominant at higher temperature are $\Delta H^\ddagger = 9.4\text{ kcal/mol}$, $\Delta S^\ddagger = -4.9\text{ cal/(mol K)}$, and $\Delta G^\ddagger_{298} = 10.8\text{ kcal/mol}$. The coalescence temperatures observed for these processes are $-30\text{ }^\circ\text{C}$ (seen in the OCH_3 , CH_3 , and $\eta^6\text{-C}_6\text{Me}_6$ resonances) and $-35\text{ }^\circ\text{C}$ (seen in the vinyl proton resonances of DPVP), which give ΔG^\ddagger_c values of approximately 11.0 and 10.8 kcal/mol , respectively. Proton NOE experiments at $-80\text{ }^\circ\text{C}$ show spin-saturation transfer rather than NOE enhancements upon irradiation of any resonance in the spectrum (see Figure 5), indicating that the molecule continues to be dynamic even at low temperatures. One would not expect to see large-magnitude negative NOE values for compounds

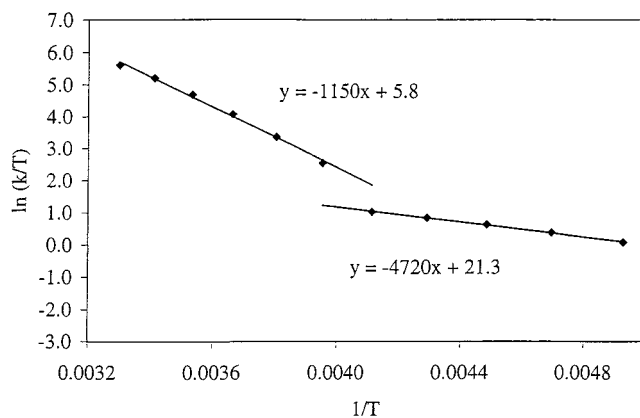


Figure 4. Eyring plot of the temperature dependence of the two-site exchange processes seen to occur in the OCH_3 resonance of $[(\eta^6\text{-C}_6\text{Me}_6)\text{Cl}(\text{DPVP})\text{Ru}=\text{C}(\text{OCH}_3)\text{CH}_3]\text{PF}_6$ (**3a**). Temperatures $-30\text{ }^\circ\text{C}$ and above were treated by analysis of line widths; temperatures $-40\text{ }^\circ\text{C}$ and below were treated by analysis of the chemical shift differences.

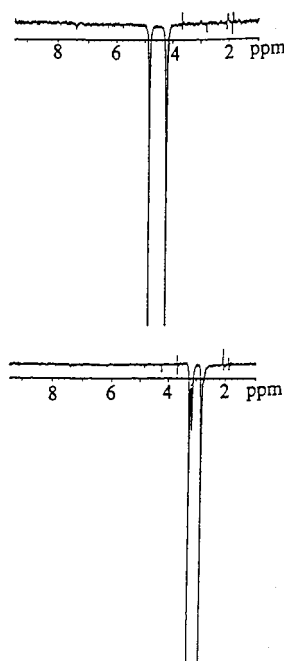


Figure 5. Low-temperature ($-80\text{ }^\circ\text{C}$) ^1H NOE experiments on $[(\eta^6\text{-C}_6\text{Me}_6)\text{Cl}(\text{DPVP})\text{Ru}=\text{C}(\text{OCH}_3)\text{CH}_3]\text{PF}_6$ (**3a**). Irradiation of one of the OCH_3 resonances shows complete spin-saturation transfer to the other OCH_3 resonance (top). Irradiation of one of the CH_3 resonances shows complete spin-saturation transfer to the other CH_3 resonance (bottom).

this small, and in any case proton–proton NOE's cannot exceed 50%. Thus, Figure 5 clearly demonstrates spin saturation transfer due to chemical exchange rather than NOE effects. We have (somewhat arbitrarily) assigned the higher energy process to hindered rotation about the $\text{Ru}-\text{P}$ bond. Similarly, we have assigned the lower energy process to hindered rotation about the $\text{Ru}-\text{C}$ bond. This is suggestive of a fair contribution from canonical forms **II** and/or **III** and a steric contribution from the bulk of the DPVP ligand.

The $^{31}\text{P}\{^1\text{H}\}$ VT NMR spectral data for **4a** have been analyzed by an Eyring plot and show only one dynamic process with activation parameters of $\Delta H^\ddagger = 5.5\text{ kcal/mol}$, $\Delta S^\ddagger = -20.0\text{ cal/(mol K)}$, and $\Delta G^\ddagger_{298} = 11.5\text{ kcal/mol}$.

Table 5. Rotational Barriers (kcal/mol) and Dihedral Angles (deg) for $[(\eta^6\text{-C}_6\text{Me}_6)\text{Cl}(\text{PR}_3)\text{Ru}=\text{C}(\text{OCH}_3)\text{R}']\text{PF}_6$

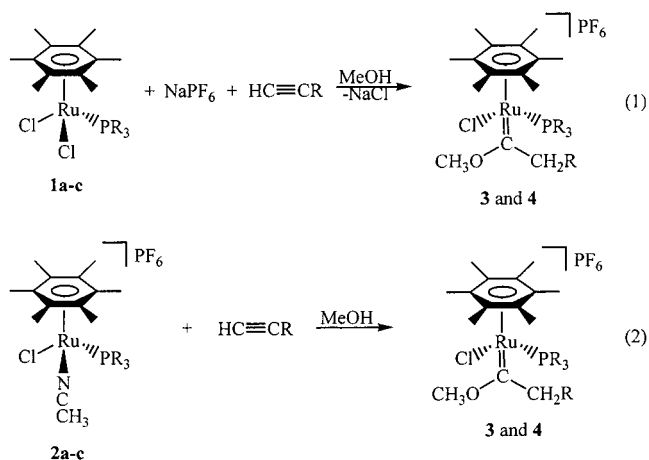
	PR ₃	R'	Ru=C (ΔG^\ddagger)	Ru-P (ΔG^\ddagger)	dihedral angle
3a	DPVP	CH ₃	$\Delta G^\ddagger_{298} = 10.8$	$\Delta G^\ddagger_{298} = 12.8$	79.9
4a	DPVP	CH ₂ Ph	free rotation	$\Delta G^\ddagger_{298} = 11.5$	37.9
3b	PMe ₃	CH ₃	free rotation	free rotation	78.1
4b	PMe ₃	CH ₂ Ph	free rotation	free rotation	59.6
3c	PPh ₃	CH ₃	free rotation	$\Delta G^\ddagger_{273} \approx 12.5$	92.3
4c	PPh ₃	CH ₂ Ph	free rotation	$\Delta G^\ddagger_{248} \approx 11$	57.7

mol. We attribute this dynamic behavior to hindered rotation about the Ru–P bond.

The PPh₃ complexes **3c** and **4c** also show only one dynamic process between +25 and –90 °C, and the ¹³C-{¹H} VT NMR very clearly demonstrates that process to be hindered rotation about the Ru–P bond. Low-temperature ¹³C-{¹H} NMR spectra of both compounds show three sets of resonances each for the *ipso*, *ortho*, *meta*, and *para* carbons of the phenyl rings. In the spectra of complex **3c** at –60 °C, the P–C coupling constants are resolved (see the Experimental Section). The ¹H variable-temperature NMR spectra also show this phenomenon in the 7–8 ppm region for the PPh₃ protons of both **3c** and **4c**. From the ¹H NMR spectra, the coalescence temperatures are estimated to be 0 °C for **3c** and –25 °C for **4c**, giving $\Delta G^\ddagger_{273} \approx 12.5$ kcal/mol for **3c** and $\Delta G^\ddagger_{248} \approx 11$ kcal/mol for **4c**. No splitting of the $\eta^6\text{-C}_6\text{Me}_6$, OCH₃, CH₃, or CH₂ resonances was seen above –90 °C. This observation can be explained by taking into account steric contributions (PPh₃ was the largest phosphine studied) and electronic contributions (forms **II** and/or **III**). Data for the six carbene complexes are collected in Table 5.

Both reviewers have suggested that the dynamic behavior of **3a** could be a result of hindered rotation about the C–O bond due to the dominance of form **III**, as previously reported for $[(\eta^5\text{-C}_5\text{Me}_5)\text{Ru}(\text{CO})_2(\text{CHOCH}_3)]\text{-PF}_6$.^{13e} We believe that this is not the case for the following reasons. For **3a** the dynamic behavior is clearly a reversible process, whereas that for $[(\eta^5\text{-C}_5\text{Me}_5)\text{Ru}(\text{CO})_2(\text{CHOCH}_3)]\text{PF}_6$ is irreversible. No NOE is observed at –80 °C between the CH₃ and OCH₃ resonances. Such NOE would be expected for hindered CO rotation. Further, the $\eta^6\text{-C}_6\text{Me}_6$ CH₃ resonance splits into two resonances at low temperature. For a freely rotating $\eta^6\text{-C}_6\text{Me}_6$ moiety parallel to the plane of the two isomers of a methoxymethylcarbene group (which should be the more stable geometry), only one $\eta^6\text{-C}_6\text{Me}_6$ CH₃ resonance should be observed.

Comparison of Reaction Routes: $1a\text{--}c + \text{NaPF}_6 \rightarrow \text{Methoxyalkylcarbenes (Eq 1)}$ or $2a\text{--}c \rightarrow \text{Methoxyalkylcarbenes (Eq 2)}$. Complex **4a** was prepared in 51% yield directly from **1a** with NaPF₆ and HC≡CPh in a MeOH/CH₂Cl₂ mixture. As we predicted (vide supra), complexes **4a** and **3b** were formed in higher yields by starting with the cationic complexes **2a,b** than by starting with the neutral complexes **1a,b** and NaPF₆: **2a** → **4a** (78%) vs **1a** → **4a** (51%) and **2b** → **3b** (100%) vs **1b** → **3b** (61%).^{9a} However, this was not the case for the preparations of **3c** and **4b,c**. (The preparation of **3a** was not attempted from **1a** after it was produced in 90% yield starting with **2a**.) The reactions of **2a–c** appear to be slower than those of **1a–c** and NaPF₆, as determined by ³¹P{¹H} NMR spectroscopic monitoring of reaction progress. For example, the



formation of **4a** from **1a** is nearly complete in ~1.5 h but takes 24 h from **2a** (see Experimental Section), and **4b,c** are reportedly formed in 10–30 min from **1b,c**^{9a} but take more than 1 day from **2b,c**. As mentioned earlier, the acetonitrile complexes are not indefinitely stable in solution, and we have found that impure solutions of all of the carbene complexes slowly decompose in solution (i.e., upon crystallization attempts),¹⁶ the PPh₃ complexes being especially unstable. From the reactions with **2a–c** we saw evidence (¹H and ¹³C-{¹H} NMR and IR) for the formation of Ru–carbonyl species. (We also isolated a small amount of $[(\eta^6\text{-C}_6\text{Me}_6)\text{Cl}(\text{PPh}_3)\text{-Ru}(\text{CO})]\text{PF}_6$ as red crystals from a prolonged reaction of **1c** with HC≡CPh and NaPF₆.) These observations indicate that beginning with complexes **2a–c** is not the most favorable route to choose.

The carbonyl species observed most probably resulted from attack on an intermediate vinylidene species by adventitious water in the reaction solvents (MeOH and CH₂Cl₂) by a previously described mechanism. The first step is coordination of the alkyne to the site on the metal vacated by CH₃CN. This probably occurs initially in an η^2 -alkyne fashion with facile conversion to the η^1 -vinylidene species, as postulated¹⁷ for several metal complexes. The α -carbon of late-transition-metal vinylidenes is readily attacked by nucleophiles,^{9,11a} including water,¹⁸ to give disubstituted carbenes. Hydroxycarbenes can undergo β -hydride elimination followed by reductive elimination of an organic molecule to give the carbonyl species. Each of these types of species have been isolated from similar reactions by many groups.^{9,11a,17–19}

The ¹³C-{¹H} NMR spectra for $[(\eta^6\text{-C}_6\text{Me}_6)\text{ClRu}(\text{PR}_3)(\text{CO})]\text{PF}_6$ show the carbonyl carbon resonances as doublets at ~195 ppm with two-bond P–C coupling constants of ~25 Hz. Infrared spectroscopy shows $\nu(\text{CO})$ stretching vibrations at ~2013 cm^{–1}. All other spectral data are as expected (see Experimental Section).

Synthesis and Characterization of the Oxacyclic Carbene $[(\eta^6\text{-C}_6\text{Me}_6)\text{Cl}(\text{DPVP})\text{Ru}=\text{C}(\text{CH}_2\text{CH}_2\text{CH}_2\text{O})]\text{-}$

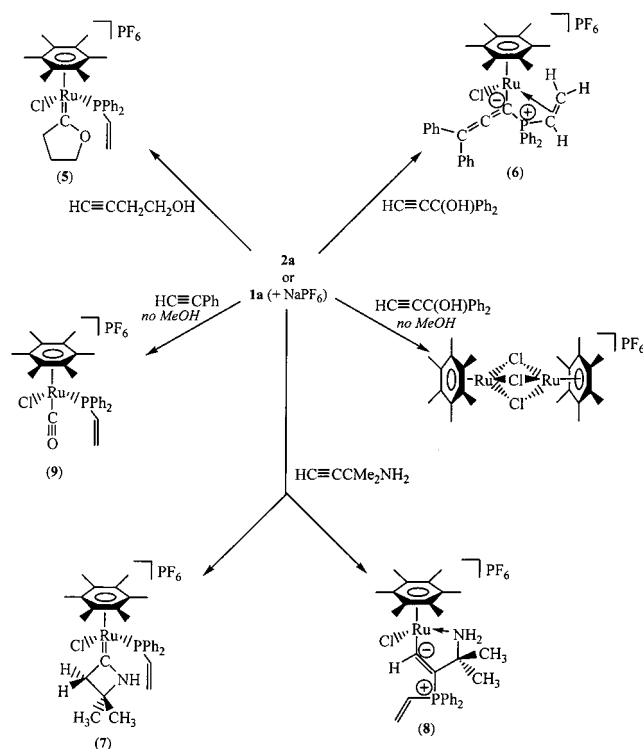
(16) Dixneuf and co-workers have stated that complexes **4b,c** are “stable methoxybenzylcarbene-ruthenium complexes”, but they do not specify whether as solids or in solution (see ref 9a, p 2769).

(17) Bruce, M. I. *Chem. Rev.* **1991**, 91, 197.

(18) (a) Davies, S. G.; McNally, J. P.; Smallridge, A. J. *Adv. Organomet. Chem.* **1990**, 30, 1. (b) Gamasa, M. P.; Gimeno, J.; Lastra, E.; Lanfranchi, M.; Tiripicchio, A. *J. Organomet. Chem.* **1992**, 430, C39. (c) Bruce, M. I.; Swincer, A. G. *Aust. J. Chem.* **1980**, 33, 1471.

(19) Bianchini, C.; Casares, J. A.; Peruzzini, M.; Romerosa, A.; Zanolini, F. *J. Am. Chem. Soc.* **1996**, 118, 4585.

Scheme 3. Novel Reactions of 1a and 2a with Terminal Alkynes



PF₆ (5). A CH₂Cl₂ solution of **1a** was treated with 1 equiv of NaPF₆ and 5 equiv of 3-butyne-1-ol and stirred overnight. The solution was filtered to remove NaCl, and the volume of the filtrate was reduced in vacuo. Addition of Et₂O produced [(η⁶-C₆Me₆)Cl(DPVP)Ru=C(CH₂)₃O]PF₆ (**5**) as an air-stable yellow powder in 71% yield after recrystallization (see Scheme 3).

The cyclic oxycarbene is evidenced by the resonances at 313.25 (²J(PC) = 14.0 Hz), 88.58, 21.13, and 55.78 ppm for the carbene and CH₂ carbons, respectively, in the ¹³C{¹H} NMR spectrum. Similar cyclic oxycarbenes show these resonances at 317.38 (²J(PC) = 22.0 Hz), 87.98, 21.54, and 55.96 ppm for [(η⁶-C₆Me₆)Cl(PMe₃)Ru=C(CH₂)₃O]PF₆^{4a} and 299.50 (²J(PC) not resolved), 80.86, 23.41, and 55.81 ppm for [(η⁵-C₅Me₅)(DPVP)₂Ru=C(CH₂)₃O]PF₆.² The -(CH₂)₃- protons resonate as multiplets between 5.2 and 1.5 ppm, similar to what is reported for other cyclic oxycarbenes.^{2,9a,20} The characteristic multiplets for the vinyl protons in **5** are seen at 6.63, 6.11, and 5.41 ppm.

Complex **5** was characterized by X-ray crystallography, and a view of the cation is shown in Figure 6. Selected bond distances and angles are listed in Table 6. Analysis shows a distorted-octahedral structure about Ru with the η⁶-C₆Me₆ ligand occupying three facial coordination sites. The three remaining ligands (Cl, DPVP, and carbene) complete the coordination sphere. The Ru=C(carbene) bond length of 1.958(7) Å is similar to the Ru=C bond length found for the Ru=C(carbene) of [(η⁵-C₅Me₅)(DPVP)₂Ru=C(CH₂)₃O]⁺ (1.942 Å).² The

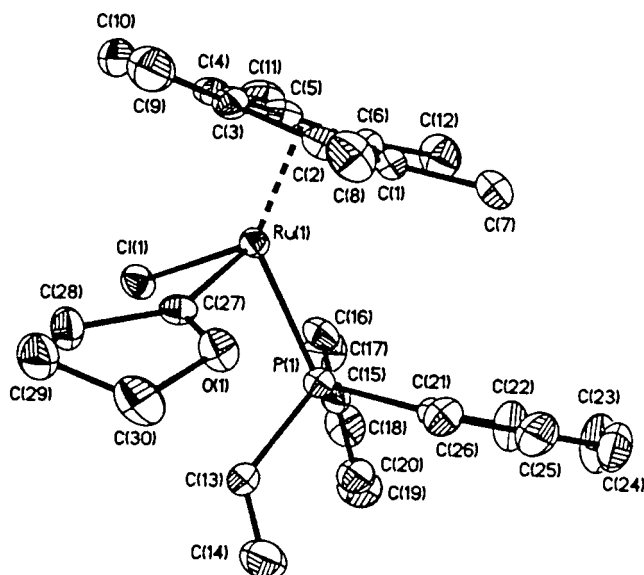


Figure 6. Structural drawing of the cation of [(η⁶-C₆Me₆)Cl(DPVP)Ru=C(CH₂)₃O]PF₆ (**5**) showing the atom-numbering scheme (30% probability ellipsoids). Hydrogen atoms have been omitted for clarity.

Table 6. Selected Bond Distances (Å) and Angles (deg) for [(η⁶-C₆Me₆)Cl(DPVP)Ru=C(CH₂)₃O]PF₆ (5**)**

Distances			
Ru(1)–C(27)	1.958(7)	C(27)–C(28)	1.495(9)
Ru(1)–P(1)	2.339(2)	C(27)–O(1)	1.308(8)
Ru(1)–Cl(1)	2.396(2)	C(28)–C(29)	1.512(9)
Ru(1)–C(arene) (av)	2.297(8)	C(29)–C(30)	1.486(11)
C(13)–C(14)	1.258(10)	C(30)–O(1)	1.466(8)
Angles			
C(27)–Ru(1)–Cl(1)	88.1(2)	Ru(1)–C(27)–O(1)	122.3(5)
C(27)–Ru(1)–P(1)	87.1(2)	Ru(1)–C(27)–C(28)	129.8(5)
Cl(1)–Ru(1)–P(1)	85.63(7)	C(28)–C(27)–O(1)	107.9(6)

five-membered ring showed the typical puckered-envelope conformation with deviations from planarity of +0.0609 (C(27)), −0.1445 (C(28)), +0.1731 (C(29)), −0.1400 (C(30)), and +0.0505° (O(1)).

Unexpected Synthesis of a Novel Phosphorus Ylide. In an attempt to prepare a vinylcarbene complex similar to [(η⁶-C₆Me₆)RuCl(PMe₃)=C(OCH₃)CH=CRR']PF₆,^{9d} complex **1a** was reacted with 1 equiv of NaPF₆ and 5 equiv of 1,1-diphenylprop-3-yn-1-ol, HC≡CC(OH)Ph₂, in 1:1 MeOH/CH₂Cl₂. The solution quickly turned from red-orange to dark red to nearly black. After 24 h of stirring at room temperature, the solvent volume of the dark red solution was reduced in vacuo. Addition of Et₂O caused the precipitation of an orange powder that was identified by ¹H and ³¹P{¹H} NMR spectroscopy as the starting material (**1a**). After several such precipitations of starting material, the novel ylide complex [(η⁶-C₆Me₆)ClRuC(=C=CPh₂)PPh₂CH=CH₂]PF₆ (**6**) was obtained as impure oily red crystals in 16% yield. Alternatively, the reaction of complex **2a** and HC≡CC(OH)Ph₂ in MeOH/CH₂Cl₂ produced complex **6** in 24% yield, also as impure oily red crystals. The structure of **6** was established by X-ray crystallography.

Two views of the cation of **6** are shown in Figure 7: the first is of the entire cation; the phenyl groups, except for the *ipso* carbons, have been removed for clarity in the second view. Table 7 lists selected bond distances

(20) (a) Bruce, M. I.; Swincer, A. G.; Thomson, B. J.; Wallis, R. C. *Aust. J. Chem.* **1980**, *33*, 2605. (b) Gamasa, M. P.; Gimeno, J.; Gonzalez-Cueva, M.; Lastra, E. *J. Chem. Soc., Dalton Trans.* **1996**, 2547.

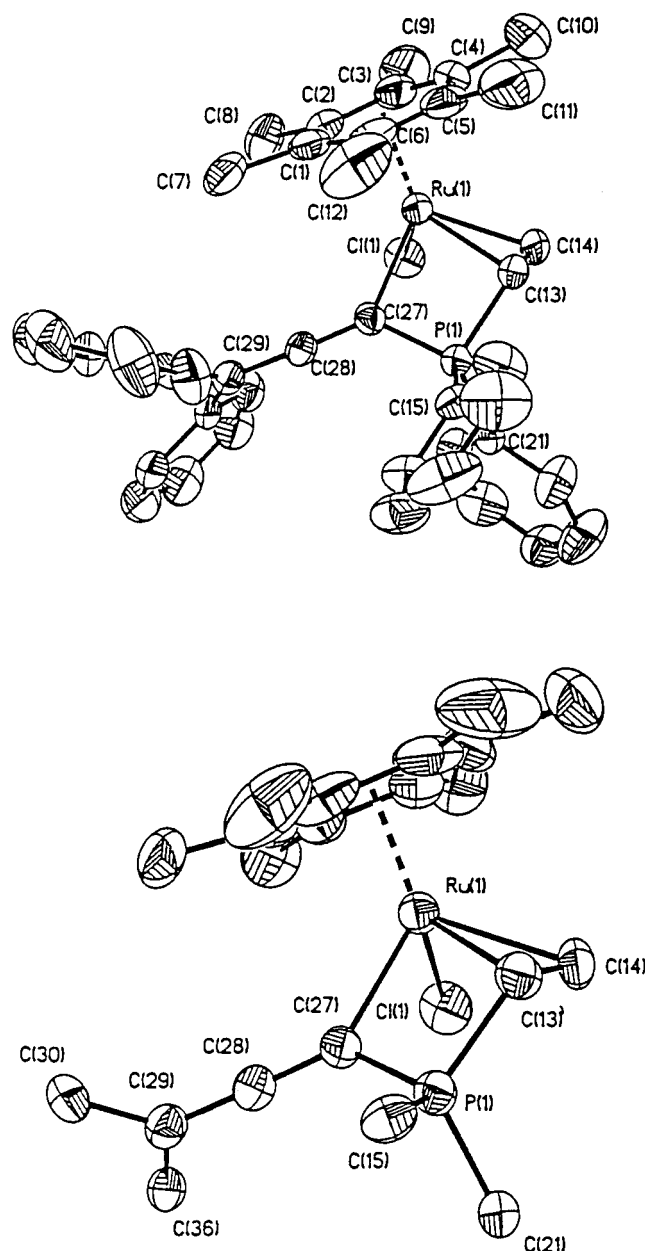


Figure 7. Structural drawings of the cation of $[(\eta^6\text{-C}_6\text{Me}_6)\text{ClRuC(=C=CPh}_2\text{)PPh}_2\text{CH=CH}_2]\text{PF}_6$ (**6**) showing the full atom-numbering scheme (top, 30% probability ellipsoids) and the unique central geometry of the ylide (bottom; phenyl ring carbons, except C_1 , have been omitted for clarity; 40% probability ellipsoids). Hydrogen atoms have been omitted for clarity in both views.

and angles. The Ru atom is in a distorted-octahedral geometry, with the $\eta^6\text{-C}_6\text{Me}_6$ ligand occupying one face and the Cl, allenyl, and vinyl ligands occupying the three sites of the opposite face. Of particular significance are the Ru–P separation, the vinyl C=C bond length, the Ru–C(27) bond length, and the allenyl geometry. The Ru–P separation of 2.902(2) Å is quite a bit longer than the sum of the atomic radii of Ru and P (1.32 and 1.10 Å, respectively), indicating the absence of a bonding interaction between Ru and P. The C(13)–C(14) bond is slightly elongated (1.395(11) vs 1.258–1.289 Å for the uncoordinated vinyl of DPVP) due to σ -donation to Ru from the C=C π molecular orbital and π -back-donation of electron density from ruthenium into the C=C π^* -

Table 7. Selected Bond Distances (Å) and Angles (deg) for

$[(\eta^6\text{-C}_6\text{Me}_6)\text{ClRuC(=C=CPh}_2\text{)PPh}_2\text{CH=CH}_2]\text{PF}_6$ (**6**)

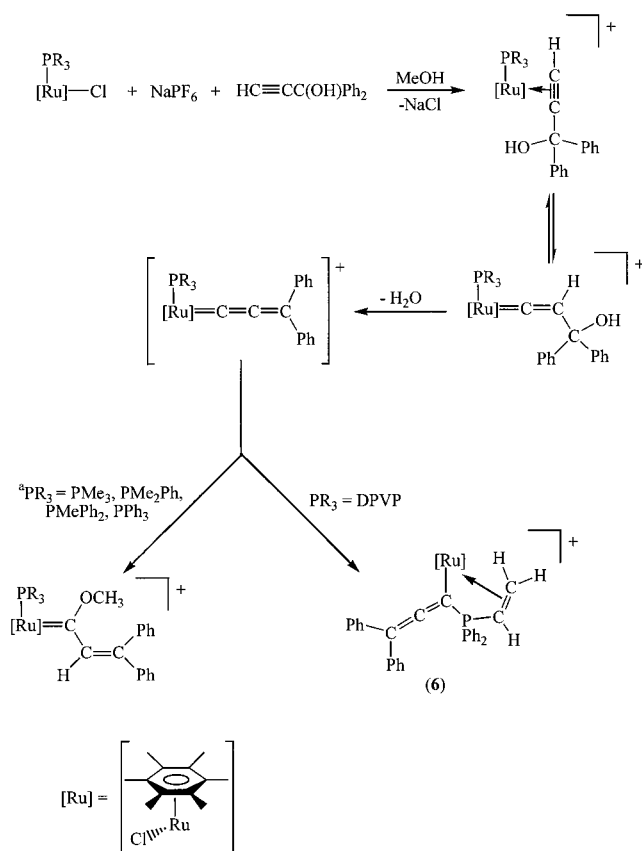
Distances			
Ru(1)–C(27)	2.122(7)	C(13)–C(14)	1.395(11)
Ru(1)–P(1)	2.902(2)	C(27)–C(28)	1.289(9)
Ru(1)–Cl(1)	2.396(2)	C(28)–C(29)	1.319(9)
Ru(1)–C(arene) (av)	2.270(9)	C(27)–P(1)	1.758(7)
Ru(1)–C(13)	2.193(7)	P(1)–C(13)	1.782(7)
Ru(1)–C(14)	2.185(7)		
Angles			
C(27)–Ru(1)–Cl(1)	83.9(2)	Ru(1)–C(27)–P(1)	96.4(3)
C(27)–Ru(1)–C(13)	74.6(3)	Ru(1)–C(27)–C(28)	134.1(6)
C(27)–Ru(1)–C(14)	97.2(3)	C(28)–C(27)–P(1)	129.5(6)
C(13)–Ru(1)–C(14)	37.2(3)	C(27)–C(28)–C(29)	178.5(7)
Cl(1)–Ru(1)–C(13)	108.1(2)	C(28)–C(29)–C(30)	119.2(7)
Cl(1)–Ru(1)–C(14)	81.8(2)	C(28)–C(29)–C(36)	119.3(7)
C(27)–P(1)–C(13)	95.3(3)	C(30)–C(29)–C(36)	121.4(6)
C(27)–P(1)–C(15)	115.1(3)	P(1)–C(13)–C(14)	119.7(6)
C(27)–P(1)–C(21)	113.1(3)	P(1)–C(13)–Ru(1)	93.2(3)
C(15)–P(1)–C(21)	108.1(3)	C(14)–C(13)–Ru(1)	71.1(4)
C(13)–P(1)–C(21)	113.6(3)		

antibonding molecular orbital. Similar C=C bond elongation upon metal coordination is seen for the Cp and Cp* complexes $[(\eta^5\text{-C}_5\text{H}_5)\text{Ru}(\eta^1\text{-DPVP})(\eta^3\text{-DPVP})]\text{PF}_6$ ¹ and $[(\eta^5\text{-C}_5\text{Me}_5)\text{Ru}(\eta^1\text{-DPVP})(\eta^3\text{-DPVP})]\text{PF}_6$,² in which one of the vinyl groups is coordinated to ruthenium. The C=C bond distances are 1.399(5)¹ and 1.51(3) Å² for the η^3 -DPVP ligands and 1.306(5)¹ and 1.24(2) Å² for the η^1 -DPVP ligands. The Ru–C(27) bond distance of 2.122(7) Å is indicative of a Ru–C(sp²) single bond, rather than a Ru=C(sp²) double bond, and is similar to the Ru–C(sp²) distance reported for $(\eta^5\text{-C}_5\text{H}_5)(\text{CO})(\text{PPr}^i_3)\text{RuC}(\text{PPh}_2)=\text{C}=\text{CPh}_2$ (2.139(5) Å).^{21a} The C(27)–C(28) and C(28)–C(29) bond distances (1.289(9) and 1.319(9) Å, respectively) and the C(27)–C(28)–C(29) angle (178.5(7)°) support an allenyl formulation. They are similar to the metrical parameters reported by Esteruelas and co-workers^{21a} for $(\eta^5\text{-C}_5\text{H}_5)(\text{CO})(\text{PPr}^i_3)\text{RuC}(\text{PPh}_2)=\text{C}=\text{CPh}_2$. Finally, as can be seen from Figure 7, the phosphorus atom has tetrahedral geometry, with the average angle about P being 109°. The unusual phosphorus ylide in this complex is stabilized in its dipolar form by coordination to ruthenium.

In the ¹H NMR spectrum, the resonances for the protons of the vinyl group have been shifted significantly upfield (4.06 to 3.69 ppm) from those of uncoordinated vinyl protons (typically 7.0 to 5.3 ppm for cationic arene–Ru complexes³). This confirms the decreases in C=C bond order and in deshielding upon η^2 -coordination to ruthenium. Similarly, the vinyl carbon resonances are seen at 28.35 ppm (¹J(PC) = 88.1 Hz) and 66.5 ppm vs the normal 130–135 ppm range. The carbons of the allenyl chain resonate at 89.92, 204.94, and 111.70 ppm (C(27), C(28), and C(29) in Figure 7). For similar ylide (or allenyl–phosphonio) complexes,²¹ the same carbon resonances are found at 71–84, 210–217, and 101–104 ppm, respectively. The IR spectrum contains the characteristic C=C=C stretch at 1976 cm^{−1} and CH=CH₂ stretch at 1448 cm^{−1}.

Complex **6** most probably resulted from intramolecular attack of the coordinated DPVP phosphorus on C_α

(21) (a) Esteruelas, M. A.; Gómez, A. V.; López, A. M.; Modrego, J.; Oñate, E. *Organometallics* **1998**, *17*, 5434. (b) Cadierno, V.; Gamasa, M. P.; Gimeno, J.; López-González, M. C.; Borge, J.; García-Granda, S. *Organometallics* **1997**, *16*, 4453.

Scheme 4. Proposed Mechanism for Formation of the Novel Ylide Complex 6^a Reference 9a.

of the allenylidene intermediate postulated in reactions of $(\eta^6\text{-C}_6\text{Me}_6)\text{RuCl}_2(\text{PR}_3)$ complexes with $\text{HC}\equiv\text{CC(OH)Ph}_2$,^{9d} rather than the expected intermolecular attack by MeOH (Scheme 4). This attack is facilitated by the ability of the vinyl group to coordinate to Ru in an η^2 fashion. This coordination behavior of the vinyl group in DPVP was previously demonstrated by Nelson and co-workers in the bisphosphine complexes $[(\eta^5\text{-C}_5\text{H}_5)\text{-Ru}(\eta^1\text{-DPVP})(\eta^3\text{-DPVP})]\text{PF}_6$ ¹ and $[(\eta^5\text{-C}_5\text{Me}_5)\text{-Ru}(\eta^1\text{-DPVP})(\eta^3\text{-DPVP})]\text{PF}_6$ ² already discussed.

Reaction with an Aminoalkyne, 1,1-Dimethyl-2-propargylamine. We next attempted a reaction for which we have seen no direct precedent—that of **1a** or **2a** with an aminoalkyne (rather than an hydroxyalkyne). We anticipated the formation of a methoxy-(aminoethyl)carbene ($\{\text{Ru}\}=\text{C(OCH}_3\text{)CH}_2\text{CMe}_2\text{NH}_2$) or, with excess aminoalkyne behaving as a base, deprotonation^{10b,22} of a vinylidene to form an (aminoalkynyl)-ruthenium complex ($\{\text{Ru}\}-\text{C}\equiv\text{CCMe}_2\text{NH}_2$). Instead, we have isolated two other complexes. Reaction of **2a** with excess dimethylpropargylamine in MeOH/ CH_2Cl_2 at room temperature for 30.5 h gave less than 10% isolated yield of the cyclic aminocarbene $[(\eta^6\text{-C}_6\text{Me}_6)\text{Cl}(\text{DPVP})\text{-Ru}=\text{CCH}_2\text{CMe}_2\text{NH}]\text{PF}_6$ (**7**), whose identity was confirmed by an X-ray crystal structure determination that gave a poor data set but sufficient information to establish bond connectivities (refer to Scheme 3 for a structural drawing). Reaction of **1a** and NaPF₆ with 1

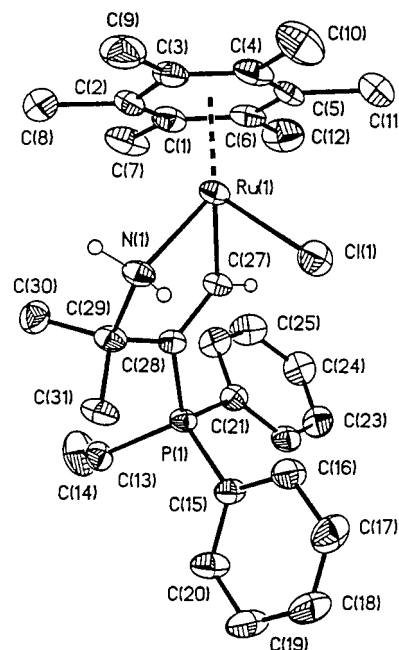


Figure 8. Structural drawing of the cation of $[(\eta^6\text{-C}_6\text{Me}_6)\text{-ClRuCH}=\text{C}(\text{DPVP})\text{CMe}_2\text{NH}_2]\text{PF}_6$ (**8**) showing the atom-numbering scheme (30% probability ellipsoids). Hydrogen atoms on C(27) and N(1) are in calculated positions and have an arbitrary radius of 1 Å. All other hydrogen atoms have been omitted for clarity.

equiv of aminoalkyne in refluxing CH_2Cl_2 or with 4 equiv of aminoalkyne in refluxing dichloroethane gave starting material, complex **7** (<10% yield), and the

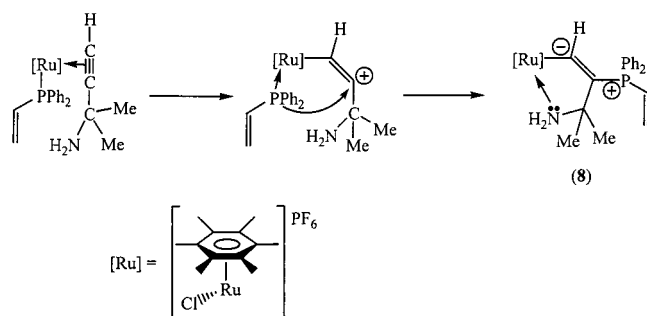
ruthenacycle $[(\eta^6\text{-C}_6\text{Me}_6)\text{ClRuCH}=\text{C}(\text{DPVP})\text{CMe}_2\text{NH}_2]\text{PF}_6$ (**8**; <10% yield), also characterized initially by an X-ray structural determination (Figure 8). Complexes **7** and **8** have not-too-different structures (e.g., both are cyclic complexes and both have a dangling rather than a chelating vinylphosphine). For complex **7**, the geminal CH_2 protons next to the carbene carbon are found as a singlet at 1.25 ppm, and the *gem*-dimethyl protons are found as a singlet at 1.76 ppm in the ^1H NMR spectrum. The observance of singlets rather than separate, coupled resonances is indicative of nitrogen inversion within the ring that causes the diastereotopic protons to be chemical shift equivalent. Also, there is only one resonance in the $^{13}\text{C}\{^1\text{H}\}$ NMR spectrum for the *gem*-dimethyl carbon atoms (15.11 ppm). The singlet resonance at 1.42 ppm in the ^1H NMR spectrum was assigned to the NH proton on the basis of integration and the fact that it is not present in the HETCOR spectrum.

For complex **8**, the CH proton attached to Ru ($\text{Ru}-\text{CH}=\text{C}$) gives rise to a downfield chemical shift (9.73 ppm) that was assigned by its integration and P–H coupling constant (24.0 Hz). Similar to complex **7**, the *gem*-dimethyl protons are chemical shift equivalent, and they give rise to a singlet at 1.33 ppm. Their attached carbon atoms are also chemical shift equivalent (30.95 ppm). The diastereotopic NH_2 protons are found at 4.84 and 4.19 ppm with an H–H coupling constant of 10.5 Hz, indicating a strong Ru–N bond in solution as well as in the solid state. One of these protons is also long-range-coupled to phosphorus ($^4J(\text{PH}) = 4.5$ Hz). The vinyl protons for both complexes resonate in the expected downfield region (7.3–6.2 ppm). There is a

(22) Antonova, A. B.; Ioganson, A. A. *Russ. Chem. Rev. (Engl. Transl.)* **1989**, *58*, 693 and references therein.

Table 8. Selected Bond Distances (Å) and Angles (deg) for

[(η^6 -C ₆ Me ₆)ClRuCH=C(DPVP)CMe ₂ NH ₂] ⁺ PF ₆ ⁻ (8)			
Distances			
Ru(1)–C(27)	2.020(7)	C(28)–C(29)	1.521(10)
Ru(1)–Cl(1)	2.402(2)	C(29)–N(1)	1.515(9)
Ru(1)–C(arene) (av)	2.220(8)	N(1)–Ru(1)	2.133(6)
C(27)–C(28)	1.337(10)	C(28)–P(1)	1.789(7)
Angles			
C(27)–Ru(1)–Cl(1)	84.9(2)	C(27)–C(28)–C(29)	119.2(6)
C(27)–Ru(1)–N(1)	76.5(3)	P(1)–C(28)–C(29)	120.8(5)
N(1)–Ru(1)–Cl(1)	82.59(19)	C(28)–C(29)–N(1)	103.3(6)
C(29)–N(1)–Ru(1)	116.3(4)	C(27)–C(28)–P(1)	120.0(6)
Ru(1)–C(27)–C(28)	119.9(5)		

Scheme 5. Proposed Mechanism for Formation of the Ruthenacycle **8**

difference in the $^{31}\text{P}\{^1\text{H}\}$ chemical shifts of **7** and **8** that initially helped us determine that we indeed had produced two different complexes, a fact that was confirmed by the X-ray crystallographic determinations.

A view of the structure of the cation of complex **8** is shown in Figure 8, with selected bond lengths and angles collected in Table 8. Of note is the Ru–C(27) bond distance (2.02(7) Å), which is on the high end of Ru=C(sp²) bond lengths and on the low end of Ru–C(sp²) bond lengths. There is a double bond between C(27) and C(28), as evidenced by the bond distance of 1.337(10) Å and the 360° sum of angles about C(28) (119.2(6)° + 120.8(5)° + 120.0(6)°). The rest of the metallacyclic ring is comprised of single bonds, i.e., C(28)–C(29) (1.521(10) Å), C(29)–N (1.515(9) Å), and N–Ru (2.133(6) Å). The five-membered ring shows the typical puckered-envelope conformation with deviations from planarity of –0.0915 (Ru), +0.1513 (N), +0.0418 (C(27)), +0.0483 (C(28)), and –0.1498° (C(29)). The DPVP phosphorus is in a tetrahedral environment, with the average bond angle about phosphorus being 109.5°, and all P–C bonds show no P=C double-bond character, making this a tetravalent phosphonium center. The charges are balanced with Ru(II), neutral η^6 -C₆Me₆, anionic Cl[–], anionic alkyl (C[–]), neutral :N, cationic P⁺, and anionic PF₆[–] as counterion.

A possible mechanism for the formation of **8** is shown in Scheme 5. η^2 -Alkyne coordination is followed by a shift in electron density on the way to an η^1 -vinylidene complex. However, vinylidene formation is intercepted by P attack on the (probably transient) carbocation, followed by N coordination to the vacant coordination site on Ru.

Attempt To Synthesize an Allenylidene. An attempt to prepare either an allenylidene or the ylide **6** from the reaction of **2a** and HC≡CC(OH)Ph₂ in the absence of MeOH gave neither. The reaction of **2a** with

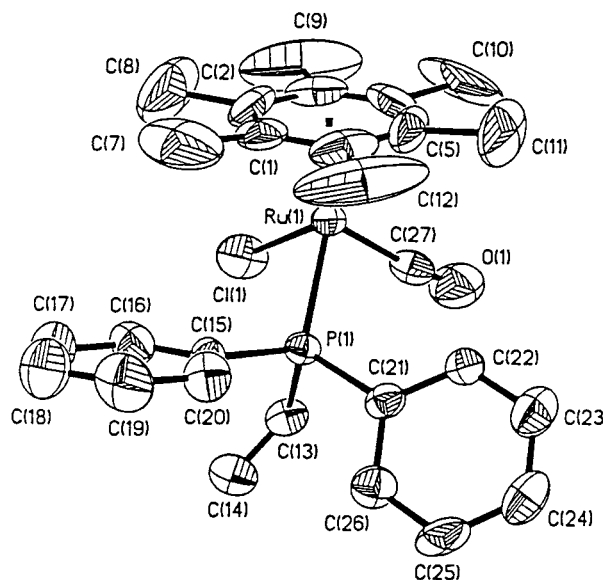


Figure 9. Structural drawing of the cation of [(η^6 -C₆Me₆)-Cl(DPVP)Ru(CO)]PF₆ (**9**) showing the atom-numbering scheme (30% probability ellipsoids). Hydrogen atoms have been omitted for clarity. Selected bond distances (Å) and angles (deg): Ru(1)–C(27), 1.933(10); Ru(1)–P(1), 2.330(2); Ru(1)–Cl(1), 2.382(2); Ru(1)–C(arene, average), 2.291(11); C(27)–O(1), 1.005(10); C(27)–Ru(1)–P(1), 86.9(3); C(27)–Ru(1)–Cl(1), 90.4(3); Cl(1)–Ru(1)–P(1), 85.45(9); Ru(1)–C(27)–O(1), 174.2(9).

1.5 equiv of HC≡CC(OH)Ph₂ in CH₂Cl₂ quickly produced a purple solution, characteristic of allenylidene species,⁹ which was stirred for 4.5 h. After this time, the solvents were removed in vacuo, and crystallization of the red-purple oil was attempted from CH₂Cl₂/Et₂O. The mixture decomposed upon recrystallization attempts, yielding only a very small amount (<10% yield based upon Ru) of the triply bridged dimer [(η^6 -C₆Me₆)Ru(μ -Cl)₃Ru(η^6 -C₆Me₆)]PF₆⁴ as fine red crystals. Apparently CH₃OH stabilizes the ylide complex **6**.

Attempt To Synthesize a Vinylidene. As in the previous synthesis, our attempt to prepare a vinylidene from **2a** and phenylacetylene in the absence of MeOH gave an unexpected product. A solution of **2a** in CH₂Cl₂ was stirred with 1 equiv of HC≡CPh for 21 days under nitrogen and gave an orange oil, crystallization of which gave the carbonyl complex [(η^6 -C₆Me₆)Cl(DPVP)Ru(CO)]PF₆ (**9**) in 11% yield. Complex **9** showed a $\nu(\text{C}=\text{O})$ vibration at 2014 cm^{–1} in its infrared spectrum and a doublet at 196.49 ppm ($^2J(\text{PC}) = 24.9$ Hz) in its $^{13}\text{C}\{^1\text{H}\}$ NMR spectrum. All aspects of the ^1H , ^{13}C –{ ^1H }, and $^{31}\text{P}\{^1\text{H}\}$ NMR spectra are as expected. An X-ray structural determination showed the familiar distorted-octahedral coordination of Ru with no unusual interionic contacts. A view of the cation is shown in Figure 9.

Electrochemistry. Complexes **3–6** and **8** were also characterized by cyclic voltammetry, and their observed Ru(II)/Ru(III) redox couples are summarized in Table 9. In both series of methoxycarbene complexes (**3a–c** and **4a–c**) the PMe₃ complexes are the easiest to oxidize, as is expected, because PMe₃ is a better σ -donor than either PPh₃ or DPVP. Dixneuf and co-workers report the Ru(II)/Ru(III) couple for **4b** at 1.15 V vs SCE,^{9a} which translates to 0.70 V vs Ag/AgCl and corrected for Fc/Fc⁺ (Fc = ferrocene) at 0.49 V. Ad-

Table 9. Electrochemical Data for Complexes 3–6 and 8^a

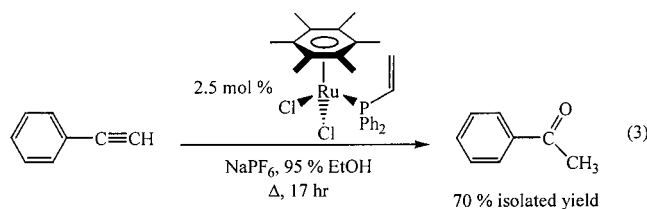
	$E_{1/2}(\text{Ru(II)/Ru(III)}), \text{ V}$	$E_{\text{p,a}} - E_{\text{p,c}}, \text{ mV}$
$[(\eta^6\text{-C}_6\text{Me}_6)\text{Cl}(\text{DPVP})\text{Ru}=\text{C}(\text{OCH}_3)\text{CH}_3]\text{PF}_6$ (3a)	0.91	183
$[(\eta^6\text{-C}_6\text{Me}_6)\text{Cl}(\text{PMe}_3)\text{Ru}=\text{C}(\text{OCH}_3)\text{CH}_3]\text{PF}_6$ (3b)	0.83	141
$[(\eta^6\text{-C}_6\text{Me}_6)\text{Cl}(\text{PPh}_3)\text{Ru}=\text{C}(\text{OCH}_3)\text{CH}_3]\text{PF}_6$ (3c)	0.96	232
$[(\eta^6\text{-C}_6\text{Me}_6)\text{Cl}(\text{DPVP})\text{Ru}=\text{C}(\text{OCH}_3)\text{CH}_2\text{Ph}]\text{PF}_6$ (4a)	0.93	189
$[(\eta^6\text{-C}_6\text{Me}_6)\text{Cl}(\text{PPh}_3)\text{Ru}=\text{C}(\text{OCH}_3)\text{CH}_2\text{Ph}]\text{PF}_6$ (4c)	0.98	170
$[(\eta^6\text{-C}_6\text{Me}_6)\text{Cl}(\text{DPVP})\text{Ru}=\text{C}(\text{CH}_2)_3\text{O}]\text{PF}_6$ (5)	0.96	134
$[(\eta^6\text{-C}_6\text{Me}_6)\text{ClRuC}(\text{C}=\text{CPh}_2)\text{PPh}_2\text{CH}=\text{CH}_2]\text{PF}_6$ (6)	0.98 ^b	
$[(\eta^6\text{-C}_6\text{Me}_6)\text{ClRuCH}=\text{C}(\text{DPVP})\text{CMe}_2\text{NH}_2]\text{PF}_6$ (8)	0.43	92
$[(\eta^6\text{-C}_6\text{Me}_6)\text{Cl}(\text{PPh}_3)\text{Ru}(\text{CO})]\text{PF}_6$	0.63 ^b	

^a Conditions: measured in CH_2Cl_2 solution with 0.1 M tetrabutylammonium hexafluorophosphate as supporting electrolyte; glassy carbon working electrode; platinum-wire auxiliary electrode; Ag/AgCl reference electrode; scan rate 250 mV/s; all potentials vs Fc/Fc^+ .

^b $E_{\text{p,a}}$ only; irreversible.

ditionally, each of these cationic carbene complexes reflects the expected decreased electron density at Ru compared to the neutral complexes **1a–c** (0.47,⁴ 0.32,⁸ and 0.47 V,⁸ respectively; vide ante). Complex **5** shows a redox couple very near the potentials of the methoxycarbene complexes and is, to the best of our knowledge, the only five-membered oxacyclic carbene complex to be electrochemically characterized. Also without reported values with which to compare are complexes **6** and **8** (irreversible oxidation at 0.98 V and $E_{1/2} = 0.43$ V, respectively). Complex **7** could not be purified enough for electrochemical measurements, and complex **9** showed no electrochemical events above the solvent current. The PPh_3 analogue of **9** showed only an oxidation wave (at 0.63 V) with no return reduction wave, again pointing to the instability of PPh_3 complexes seen throughout this research (vide ante the irreversible oxidation of **2c** and the decomposition of PPh_3 complexes reported throughout this paper).⁸

Catalysis. Tokunaga and Wakatsuki reported the successful use of $(\eta^6\text{-C}_6\text{H}_6)\text{RuCl}_2(\text{PR}_3)$ ($\text{PR}_3 = \text{PPh}_2(\text{C}_6\text{F}_5)$ and $\text{P}(3\text{-C}_6\text{H}_4\text{SO}_3\text{Na})_3$) for the anti-Markovnikov hydration of terminal alkynes.²³ By varying the PR_3 group and the amount of excess PR_3 in the reaction mixture, they selectively produced the desired aldehydes in fair yields. A preliminary experiment with complex **1a**, based upon their methods, has proven fruitful (eq 3).



Phenylacetylene was heated at reflux in 95% EtOH in the presence of 2.5 mol % of **1a** for 17 h. GC/MS and ^1H NMR spectroscopy of the extracted organic product showed the presence of acetophenone (81.4%), hexamethylbenzene (15.7%), and an as yet unidentified substance (2.9%), but no phenylacetaldehyde. Acetophenone was isolated in 70% yield based upon phenylacetylene. The inorganic fraction has yet to be fully characterized, but it does show several infrared absorption bands in the M–CO region (1967–2073 cm^{-1}). This could indicate a mechanism similar to that proposed by

Tokunaga and Wakatsuki to explain the formation of both aldehydes and ketones.²³ The presence of hexamethylbenzene in the organic product has two probable origins: loss from **1a** to form the catalytically active species or loss from **1a** during workup and vacuum distillation. Tokunaga and Wakatsuki monitored the loss of C_6H_6 from one of their Ru species (by ^1H NMR spectroscopy) and postulate that the active catalytic species in their experiments is of the type $[\text{RuCl}_2\{\text{PPh}_2(\text{C}_6\text{F}_5)\}_x]$, for which they have independent data.²³ If our catalytically active species is similar, i.e. of the type $[\text{RuCl}_2(\text{DPVP})_x]$, the presence of free $\eta^6\text{-C}_6\text{Me}_6$ in the product would be explained. Or, independent of the nature of the active catalytic species, if hexane washing and chromatography during workup did not fully remove all the Ru-containing material, $\eta^6\text{-C}_6\text{Me}_6$ could have been liberated from this material along with (or after) acetophenone as a product of the heat-induced decomposition of complex **1a**. Either route could also have led to the unidentified compound seen in the GC/MS spectrum at m/z 194.

Characterization of the inorganic species produced, optimization of reaction conditions, and reactions with other alkynes are in progress.

Summary

Two new $\eta^6\text{-C}_6\text{Me}_6$ -phosphine–Ru– CH_3CN complexes (**2b,c**) were synthesized and characterized, and their reactions with terminal alkynes were investigated. It was found that reactions of the neutral complexes $(\eta^6\text{-C}_6\text{Me}_6)\text{RuCl}_2(\text{PR}_3)$ (**1**) with terminal alkynes in the presence of NaPF_6 and MeOH to form methoxycarbene complexes generally proceed more rapidly, with fewer side products, than do reactions of the cationic complexes $[(\eta^6\text{-C}_6\text{Me}_6)\text{Cl}(\text{PR}_3)\text{Ru}(\text{NCCH}_3)]\text{PF}_6$ (**2**) with terminal alkynes in MeOH. The dynamic behavior of two series of methoxyalkylcarbene complexes (**3** and **4**) was investigated by NOE and VT NMR experiments, and the data are explained by invoking both steric and electronic arguments.

In all, 12 previously unreported complexes of ruthenium have been synthesized and characterized, including the novel complexes of a phosphorus ylide (**6**), a cyclic aminocarbene (**7**), and a nitrogen-containing ruthenacycle (**8**). $(\eta^6\text{-C}_6\text{Me}_6)\text{RuCl}_2(\text{DPVP})$ was shown to catalytically hydrate phenylacetylene to give acetophenone with no evidence for phenylacetaldehyde production.

Experimental Section

General Comments. All reactions were carried out under a nitrogen atmosphere, and workups were performed without precaution to exclude air. The complexes $(\eta^6\text{-C}_6\text{Me}_6)\text{Cl}_2\text{Ru}(\text{PR}_3)$ (PR_3 = diphenylvinylphosphine (DPVP) (**1a**),⁴ PMe_3 (**1b**),⁵ PPh_3 (**1c**)⁶) and $[(\eta^6\text{-C}_6\text{Me}_6)\text{Cl}(\text{DPVP})\text{Ru}(\text{NCCH}_3)]\text{PF}_6$ (**2a**)³ were prepared by literature methods. (Trimethylsilyl)acetylene was purchased from Lancaster, phenylacetylene, 3-buten-1-ol, and 1,1-dimethylpropargylamine were purchased from Aldrich, and 1,1-diphenyl-3-propyn-1-ol was purchased from GFS Chemicals. Acetonitrile was distilled from CaH_2 prior to use. NMR spectra were recorded on a Varian Unity Plus-500 FT NMR spectrometer operating at 500 MHz for ^1H , 125 MHz for ^{13}C , and 202 MHz for ^{31}P . Proton and carbon chemical shifts were referenced to residual solvent resonances; phosphorus chemical shifts were referenced to an external 85% aqueous solution of H_3PO_4 . All shifts to low field, high frequency are positive. NOE experiments were performed with the pulse sequence reported by Shaka and co-workers.²⁴ FT-IR spectra were recorded on a Perkin-Elmer Spectrum BX spectrometer in CH_2Cl_2 solution on NaCl windows or as Nujol mulls on CsI windows (abbreviations: shp = sharp, st = strong, m = medium, w = weak, br = broad). Cyclic voltammograms were recorded at 25 °C in freshly distilled CH_2Cl_2 containing 0.1 M tetrabutylammonium hexafluorophosphate using a BAS CV50-W voltammetric analyzer. A three-electrode system was used. The working electrode was glassy carbon, the auxiliary electrode was a platinum wire, and the reference electrode was Ag/AgCl (aqueous) separated from the cell by a Luggin capillary. The Fc/Fc^+ couple occurred at 490 mV²⁵ under the same conditions. Melting points were determined on a Mel-Temp apparatus and are uncorrected. Elemental analyses were performed by Galbraith Laboratories, Knoxville, TN.

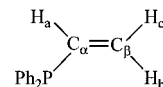
Synthesis of the Acetonitrile Complexes $[(\eta^6\text{-C}_6\text{Me}_6)\text{-Cl}(\text{PR}_3)\text{Ru}(\text{NCCH}_3)]\text{PF}_6$ (2b,c**). PR_3 = PMe_3 (**2b**).** To a red solution of $(\eta^6\text{-C}_6\text{Me}_6)\text{Cl}_2\text{Ru}(\text{PMe}_3)$ (**1b**; 0.407 g, 0.991 mmol) in 10 mL of CH_2Cl_2 was added 50 mL of CH_3CN and a solution of NaPF_6 (0.168 g, 0.997 mmol) in 10 mL of CH_3CN . The reaction mixture became cloudy within a few minutes. The mixture was stirred for 12 h and then gravity-filtered to remove NaCl . The solvents were removed in vacuo to give **2b** as a yellow powder in 86.5% yield (0.481 g); mp 195 °C. Anal. Calcd for $\text{C}_{17}\text{H}_{30}\text{ClF}_6\text{NP}_2\text{Ru}$: C, 36.39; H, 5.39; Cl, 6.32. Found: C, 36.20; H, 5.17; Cl, 6.38. IR (cm^{-1} ; Nujol): 2293 w $\nu(\text{C}\equiv\text{N})$, 843, 559 st $\nu(\text{PF}_6)$. ^1H NMR (499.84 MHz, acetone- d_6): δ 2.68 (d, $^5J(\text{PH}) = 1.5$ Hz, 3H, CH_3CN), 2.18 (d, $J(\text{PH}) = 1.0$ Hz, 18H, $\eta^6\text{-C}_6\text{Me}_6$), 1.57 (d, $^2J(\text{PH}) = 11.0$ Hz, 9H, PMe_3). $^{13}\text{C}\{^1\text{H}\}$ NMR (125.70 MHz, acetone- d_6): δ 126.99 (s, CH_3CN), 100.17 (d, $J(\text{PC}) = 2.6$ Hz, $\eta^6\text{-C}_6\text{Me}_6$), 16.21 (s, $\eta^6\text{-C}_6\text{Me}_6$), 14.98 (d, $^1J(\text{PC}) = 33.6$ Hz, PMe_3), 3.83 (s, CH_3CN). $^{31}\text{P}\{^1\text{H}\}$ NMR (202.34 MHz, acetone- d_6): δ 4.84 (s, PMe_3), -145.00 (sept, $^1J(\text{PF}) = 707.8$ Hz, PF_6).

PR_3 = PPh_3 (2c**).** Similarly, **2c** was prepared from **1c** in 27.6% yield (0.185 g), mp 180 °C dec. Anal. Calcd for $\text{C}_{32}\text{H}_{36}\text{-ClF}_6\text{NP}_2\text{Ru}$: C, 51.43; H, 4.86; Cl, 4.74. Found: C, 51.19; H, 5.01; Cl, 4.63. IR (cm^{-1} ; Nujol): 2297 w $\nu(\text{C}\equiv\text{N})$, 841 st $\nu(\text{PF}_6)$. ^1H NMR (499.84 MHz, acetone- d_6): δ 7.68–7.64 (m, 6H, Ph H_o), 7.59–7.51 (m, 9H, Ph H_m , Ph H_p), 2.22 (d, $^5J(\text{PH}) = 1.5$ Hz, 3H, CH_3CN), 1.91 (d, $J(\text{PH}) = 1.0$ Hz, 18H, $\eta^6\text{-C}_6\text{Me}_6$). $^{13}\text{C}\{^1\text{H}\}$ NMR (125.70 MHz, acetone- d_6): δ 135.54 (d, $^2J(\text{PC}) = 9.7$ Hz, C_o), 132.01 (d, $^4J(\text{PC}) = 2.3$ Hz, C_p), 129.48 (d, $^3J(\text{PC}) = 10.2$ Hz, C_m), 128.70 (s, CH_3CN), 101.64 (d, $J(\text{PC}) = 2.6$ Hz, $\eta^6\text{-C}_6\text{Me}_6$), 15.65 (s, $\eta^6\text{-C}_6\text{Me}_6$), 3.67 (s, CH_3CN). $^{31}\text{P}\{^1\text{H}\}$ NMR (202.33 MHz, acetone- d_6): δ 33.84 (s, PPh_3), -145.00 (sept, $^1J(\text{PF}) = 707.8$ Hz, PF_6).

Synthesis of the Methoxymethylcarbene Complexes $[(\eta^6\text{-C}_6\text{Me}_6)\text{Cl}(\text{PR}_3)\text{Ru}=\text{C}(\text{OCH}_3)\text{CH}_2\text{Ph}]\text{PF}_6$ (3a–c**).** To a red-

orange solution of the appropriate acetonitrile complex (**2a–c**; 0.25 g, ~0.45 mmol) in 1:1 $\text{MeOH}/\text{CH}_2\text{Cl}_2$ (10 mL) was added a 2-fold excess of (trimethylsilyl)acetylene ($\text{HC}\equiv\text{CSiMe}_3$) and the mixture was stirred for 43–49 h. The solvents were removed in vacuo, and the resulting yellow to orange powders were crystallized from $\text{CH}_2\text{Cl}_2/\text{Et}_2\text{O}$.

PR_3 = DPVP (3a**).** Reaction time: 49 h. Yield: 0.23 g (90%). Mp: 188–191 °C. Anal. Calcd for $\text{C}_{29}\text{H}_{37}\text{ClF}_6\text{OP}_2\text{Ru}$: C, 48.78; H, 5.22; Cl, 4.96. Found: C, 48.60; H, 5.17; Cl, 4.81.



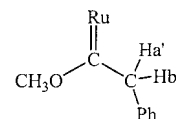
^1H NMR (499.84 MHz, CD_3NO_2): δ 7.58–7.47 (m, 10H, Ph), 6.63 (ddd, $^2J(\text{PH}) = 24.4$ Hz, $^3J(\text{H}_a\text{H}_b) = 18.3$ Hz, $^3J(\text{H}_a\text{H}_c) = 12.4$ Hz, 1H, H_a), 6.22 (dd, $^3J(\text{PH}) = 38.5$ Hz, $^3J(\text{H}_a\text{H}_c) = 12.4$ Hz, 1H, H_c), 5.48 (ddd, $^3J(\text{PH}) = 19.2$ Hz, $^3J(\text{H}_a\text{H}_b) = 18.3$ Hz, $^2J(\text{H}_b\text{H}_c) = 0.8$ Hz, 1H, H_b), 4.38 (s, 3H, OCH_3), 2.87 (s, 3H, CH_3), 1.99 (s, 18H, $\eta^6\text{-C}_6\text{Me}_6$). $^{13}\text{C}\{^1\text{H}\}$ NMR (125.71 MHz, $\text{CD}_3\text{-NO}_2$): δ 327.99 (d, $^2J(\text{PC}) = 19.9$ Hz, $\text{Ru}=\text{C}$), 134.22 (d, $^2J(\text{PC}) = 10.1$ Hz, C_o), 133.40 (d, $^2J(\text{PC}) = 9.2$ Hz, C_o), 131.25 (s, C_p), 130.98 (br s, C_p), 130.83 (s, C_p), 130.77 (d, $^1J(\text{PC}) = 51.8$ Hz, C_o), 130.77 (d, $^1J(\text{PC}) = 51.8$ Hz, C_i), 129.04 (d, $^1J(\text{PC}) = 48.8$ Hz, C_i), 128.49 (d, $^3J(\text{PC}) = 10.4$ Hz, C_m), 128.28 (d, $^3J(\text{PC}) = 10.2$ Hz, C_m), 107.38 (d, $J(\text{PC}) = 2.4$ Hz, $\eta^6\text{-C}_6\text{Me}_6$), 66.38 (s, OCH_3), 39.05 (s, CH_3), 14.91 (s, $\eta^6\text{-C}_6\text{Me}_6$). $^{31}\text{P}\{^1\text{H}\}$ NMR (202.35 MHz, CD_3NO_2): δ 31.31 (s, DPVP), -145.00 (sept, $^1J(\text{PF}) = 707.8$ Hz, PF_6).

PR_3 = PMe_3 (3b**).** Reaction time: 43 h. Yield: 0.39 g (100%). Characterization data have been reported.^{9a}

PR_3 = PPh_3 (3c**).** Reaction time: 4.5 days. Yield: $\leq 10\%$ after recrystallization. (There was enough formed to confirm formation of **3c** by NMR spectroscopy, but it was always contaminated with $[(\eta^6\text{-C}_6\text{Me}_6)_2\text{Ru}_2\text{Cl}_3]\text{PF}_6$,⁴ and impure solutions slowly decomposed in all solvents.) Complex **3c** was also formed by reaction of **1c** (0.464 g, 0.778 mmol) and NaPF_6 (0.134 g, 0.800 mmol) with $\text{HC}\equiv\text{CSiMe}_3$ (0.58 mL, 4.1 mmol) in $\text{MeOH}/\text{CH}_2\text{Cl}_2$ (1:1, 40 mL) for 24 h. Complex **3c** was isolated as yellow crystals after filtration (to remove NaCl) and crystallization from acetone/ Et_2O in 35.9% yield (0.213 g). (There was no evidence for formation of the triply chloride bridged dimer in this preparation.) Anal. Calcd for $\text{C}_{33}\text{H}_{39}\text{ClF}_6\text{-OP}_2\text{Ru}$: C, 51.87; H, 5.14; Cl, 4.64. Found: C, 51.69; H, 5.03; Cl, 4.52. ^1H NMR (499.84 MHz, acetone- d_6): δ 7.6–7.4 (br m, 15H, Ph), 4.18 (s, 3H, OCH_3), 2.91 (d, $^4J(\text{PH}) = 1.0$ Hz, 3H, CH_3), 1.93 (d, $J(\text{PH}) = 1.0$ Hz, 18H, $\eta^6\text{-C}_6\text{Me}_6$). $^{13}\text{C}\{^1\text{H}\}$ NMR (125.71 MHz, acetone- d_6): δ 331.00 (d, $^2J(\text{PC}) = 19.6$ Hz, $\text{Ru}=\text{C}$), 134.86 (br s, C_o), 131.92 (br s, C_p), 129.51 (d, $^3J(\text{PC}) = 9.2$ Hz, C_m), 108.60 (d, $J(\text{PC}) = 2.4$ Hz, $\eta^6\text{-C}_6\text{Me}_6$), 67.19 (s, OCH_3), 40.87 (d, $^3J(\text{PC}) = 1.3$ Hz, CH_3), 15.89 (s, $\eta^6\text{-C}_6\text{Me}_6$). $^{31}\text{P}\{^1\text{H}\}$ NMR (202.33 MHz, acetone- d_6): δ 38.14 (s, PPh_3), -145.00 (sept, $^1J(\text{PF}) = 708.0$ Hz, PF_6).

Synthesis of the Methoxybenzylcarbene Complexes $[(\eta^6\text{-C}_6\text{Me}_6)\text{Cl}(\text{PR}_3)\text{Ru}=\text{C}(\text{OCH}_3)\text{CH}_2\text{Ph}]\text{PF}_6$ (4a–c**).** These complexes were prepared in the same manner as complexes **3a–c** using phenylacetylene, $\text{HC}\equiv\text{CPh}$, in place of (trimethylsilyl)acetylene.

PR_3 = DPVP (4a**).** Reaction time: 24 h. Yield: 0.18 g (78%). Complex **4a** was also prepared from **1a**, NaPF_6 , and $\text{HC}\equiv\text{CPh}$ in 51% yield as described above for **3c**. Mp: 130 °C dec. Anal. Calcd for $\text{C}_{35}\text{H}_{41}\text{ClF}_6\text{OP}_2\text{Ru}$: C, 53.20; H, 5.23; Cl, 4.49. Found: C, 53.04; H, 5.31; Cl, 4.57.



^1H NMR (499.84 MHz, CDCl_3): δ 7.15–7.63 (m, 15H, Ph), 6.87 (ddd, $^2J(\text{PH}) = 23.0$ Hz, $^3J(\text{H}_a\text{H}_b) = 18.0$ Hz, $^3J(\text{H}_a\text{H}_c) = 12.3$

(24) Stott, K.; Stonehouse, J.; Keeler, J.; Hwang, T.-L.; Shaka, A. J. *J. Am. Chem. Soc.* **1995**, *117*, 4199.

(25) Gagné, R. R.; Koval, C. A.; Lisensky, G. C. *Inorg. Chem.* **1980**, *19*, 2854.

Hz, 1H, H_a), 6.19 (dd, ³J(PH) = 40.0 Hz, ³J(H_aH_c) = 12.3 Hz, 1H, H_c), 5.39 (dd, ³J(PH) = 19.5 Hz, ³J(H_aH_b) = 18.0 Hz, 1H, H_b), 5.07 (d, ²J(H_aH_b) = 12.5 Hz, 1H, H_a), 4.50 (s, 3H, OCH₃), 3.23 (d, ²J(H_aH_b) = 12.5 Hz, 1H, H_b), 1.80 (s, 18H, η⁶-C₆Me₆). ¹³C{¹H} NMR (125.71 MHz, CDCl₃): δ 314.54 (²J(PC) = 14.5 Hz, Ru=C), 134.97 (d, ²J(PC) = 10.3 Hz, C_o DPVP), 132.61 (d, ²J(PC) = 8.8 Hz, C_o DPVP), 132.14 (d, ⁴J(PC) = 2.3 Hz, C_p DPVP), 131.56 (C_i Ph), 131.34 (s, C_β), 131.09 (d, ⁴J(PC) = 2.1 Hz, C_p DPVP), 131.27 (d, ¹J(PC) = 72.9 Hz, C_o), 130.13 (s, C_o Ph), 128.90 (s, C_m Ph), 128.86 (d, ³J(PC) = 10.6 Hz, C_m DPVP), 128.63 (d, ³J(PC) = 10.3 Hz, C_m DPVP), 127.55 (s, C_p Ph), 127.00 (d, ¹J(PC) = 51.3 Hz, C_i DPVP), 109.64 (s, η⁶-C₆Me₆), 67.91 (s, OCH₃), 54.43 (s, CH₂), 15.91 (s, η⁶-C₆Me₆). ³¹P{¹H} NMR (202.33 MHz, CDCl₃): δ 27.95 (s, DPVP), -144.96 (sept, ¹J(PF) = 712.6 Hz, PF₆).

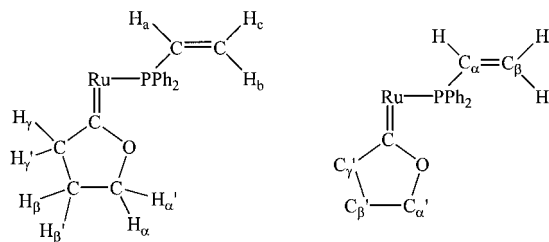
PR₃ = PMe₃ (4b). Reaction time: 93 h. Yield: ≤10%. Formation was confirmed by comparison with reported^{9a} NMR spectral data. The crude mixture decomposed to give green solutions of [(η⁶-C₆Me₆)Cl(PMe₃)Ru(CO)]PF₆ (vide infra) and free η⁶-C₆Me₆ upon crystallization attempts. Full characterization data have been reported.^{9a}

PR₃ = PPh₃ (4c). Reaction time: 11 days. Yield: ≤10%. Formation was confirmed by comparison with reported^{9a} NMR spectral data. The crude mixture decomposed to give green solutions of [(η⁶-C₆Me₆)Cl(PPh₃)Ru(CO)]PF₆ (vide infra) upon crystallization attempts. Full characterization data have been reported.^{9a}

Characterization Data for [(η⁶-C₆Me₆)Cl(PMe₃)Ru(CO)]PF₆. ¹H NMR (499.84 MHz, acetone-d₆): δ 2.61 (s, 18H, η⁶-C₆Me₆), 2.21 (d, ²J(PH) = 12.0 Hz, 9H, PMe₃). ¹³C{¹H} NMR (125.71 MHz, acetone-d₆): δ 196.64 (d, ²J(PC) = 24.6 Hz, Ru-CO), 113.38 (d, ¹J(PC) = 2.4 Hz, η⁶-C₆Me₆), 16.92 (s, η⁶-C₆Me₆), 16.23 (d, ¹J(PC) = 38.1 Hz, PMe₃). ³¹P{¹H} NMR (202.33 MHz, acetone-d₆): δ 18.68 (s, PMe₃), -139.38 (sept, ¹J(PF) = 708.8 Hz, PF₆).

Characterization Data for [(η⁶-C₆Me₆)Cl(PPh₃)Ru(CO)]PF₆. Mp: 188 °C dec. IR (cm⁻¹; CH₂Cl₂): 2012 st, sh ν(CO). ¹H NMR (499.84 MHz, acetone-d₆): δ 7.66–7.55 (m, 15H, Ph), 2.12 (d, ²J(PH) = 1.0 Hz, 18H, η⁶-C₆Me₆). ¹³C{¹H} NMR (125.71 MHz, acetone-d₆): δ 198.30 (d, ²J(PC) = 25.5 Hz, Ru-CO), 134.92 (d, ²J(PC) = 10.1 Hz, C_o), 133.06 (d, ⁴J(PC) = 2.0 Hz, C_p), 130.10 (d, ³J(PC) = 10.8 Hz, C_m), 115.33 (d, ¹J(PC) = 2.1 Hz, η⁶-C₆Me₆), 16.58 (s, η⁶-C₆Me₆). ³¹P{¹H} NMR (202.33 MHz, acetone-d₆): δ 40.47 (s, PPh₃), -145.00 (sept, ¹J(PF) = 707.6 Hz, PF₆).

Synthesis of [(η⁶-C₆Me₆)Cl(DPVP)Ru=C(CH₂)₃O]PF₆ (5). To a solution of 0.200 g (0.366 mmol) of **1a** and 0.069 g (0.369 mmol) of NaPF₆ in 40 mL of MeOH/CH₂Cl₂ (1:1, v/v) was added 0.14 mL (1.9 mmol) of 3-butyne-1-ol, HC≡CCH₂CH₂OH. After 24 h, the solvents were removed in vacuo. Filtration of a CH₂Cl₂ solution of the product removed NaCl, and crystallization from CH₂Cl₂/Et₂O gave 0.189 g (71%) of **5** as a yellow powder. Mp: 161–179 °C. Anal. Calcd for C₃₀H₃₇ClF₆OP₂Ru: C, 49.63; H, 5.14; Cl, 4.88. Found: C, 49.50; H, 4.89; Cl, 4.63.



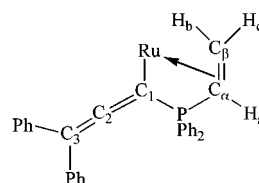
¹H NMR (499.84 MHz, CDCl₃): δ 7.42–7.54 (m, 10H, Ph), 6.63 (ddd, ³J(PH) = 22.0 Hz, ³J(H_aH_b) = 18.2 Hz, ³J(H_aH_c) = 12.2 Hz, 1H, H_a), 6.11 (dd, ³J(PH) = 39.7 Hz, ³J(H_aH_c) = 12.2 Hz, 1H, H_c), 5.41 (dd, ³J(PH) = 19.5 Hz, ³J(H_aH_b) = 18.2 Hz, 1H, H_b), 5.20 (apparent q, ²J(H_aH_c) = ³J(H_aH_b) = ³J(H_aH_β) = 8.0

Hz, 1H, H_o), 4.90 (apparent q, ²J(H_aH_c) = ³J(H_aH_β) = ³J(H_aH_β) = 8.0 Hz, 1H, H_c), 3.17 (ABXYZ, ²J(H_γH_γ) = 21.5 Hz, ³J(H_γH_β) = 9.0 Hz, ⁴J(PH) = 9.0 Hz, ³J(H_γH_β) = 5.5 Hz, 1H, H_γ), 3.07 (ABXYZ, ²J(H_γH_γ) = 21.5 Hz, ⁴J(PH) = 9.0 Hz, ³J(H_γH_β) = 8.5 Hz, ³J(H_γH_β) = 7.0 Hz, 1H, H_γ), 2.01 (m, 1H, H_β), 1.90 (s, 18H, η⁶-C₆Me₆), 1.53 (m, 1H, H_β). ¹³C{¹H} NMR (125.71 MHz, CDCl₃): δ 313.28 (d, ²J(PC) = 19.6 Hz, Ru=C), 134.15 (d, ²J(PC) = 10.2 Hz, C_o), 132.97 (d, ²J(PC) = 9.4 Hz, C_o), 131.59 (d, ⁴J(PC) = 2.5 Hz, C_p), 131.22 (br s, C_β), 131.07 (d, ⁴J(PC) = 2.3 Hz, C_p), 130.51 (d, ¹J(PC) = 47.9 Hz, C_o), 130.23 (d, ¹J(PC) = 45.6 Hz, C_i), 128.62 (d, ³J(PC) = 10.4 Hz, C_m), 128.47 (d, ³J(PC) = 10.3 Hz, C_m), 128.00 (d, ¹J(PC) = 49.8 Hz, C_i), 107.36 (d, ¹J(PC) = 2.1 Hz, η⁶-C₆Me₆), 88.46 (s, C_α), 55.75 (s, C_γ), 22.02 (s, C_β), 15.72 (s, η⁶-C₆Me₆). ³¹P{¹H} NMR (202.33 MHz, CDCl₃): δ 34.32 (s, DPVP), -145.01 (sept, ¹J(PF) = 712.2 Hz, PF₆).

Synthesis of the Novel Ylide [(η⁶-C₆Me₆)ClRuC=C=

CPh₂)PPh₂CH=CH₂]PF₆ (6). Method A. Complex **6** was prepared from 0.201 g (0.368 mmol) of **1a**, 0.061 g (0.366 mmol) of NaPF₆, and 0.381 g (1.83 mmol) of 1,1-diphenylprop-3-yn-1-ol, HC≡CC(OH)Ph₂, in 40 mL of MeOH/CH₂Cl₂ (1:1, v/v). The red-orange solution quickly became dark red, nearly black. The reaction mixture was stirred for 24 h. Reduction of the solvent volume on a rotary evaporator and addition of Et₂O precipitated starting material **1a** as an orange powder, which was collected by gravity filtration. Solvent removal from the filtrate gave a purple oil that afforded more **1a** upon repeated crystallizations from CH₂Cl₂/Et₂O. Finally, red crystals (0.048 g, 16%) of **6** were obtained from CH₂Cl₂/Et₂O.

Method B. To a solution of 0.200 g (0.288 mmol) of **2a** in 10 mL of MeOH/CH₂Cl₂ (1:1, v/v) was added 0.067 g (0.322 mmol) of HC≡CC(OH)Ph₂. The mixture was stirred for 25.5 h, after which time the solvents were removed in vacuo. The residue was washed with Et₂O and crystallized from CH₂Cl₂/Et₂O with recovery of starting material (**2a**) and decomposition predominant. Final yield: 0.028 g (24.3%). Mp: 202 °C dec. Anal. Calcd for C₄₁H₄₁ClF₆P₂Ru: C, 58.19; H, 4.88; Cl, 4.19. Found: C, 58.27; H, 4.69; Cl, 4.03. IR (cm⁻¹; CDCl₃): 1976 br, w ν(C=C=C), 1448 m ν(CH=CH₂), 846, 548 st ν(PF).



¹H NMR (499.84 MHz, CDCl₃): δ 7.89–7.05 (m, 20H, Ph), 4.06 (ddd, ³J(PH) = 19.7 Hz, ³J(H_aH_b) = 12.2 Hz, ²J(H_bH_c) = 1.6 Hz, 1H, H_b), 3.81 (ddd, ³J(PH) = 29.4 Hz, ³J(H_aH_c) = 9.6 Hz, ²J(H_bH_c) = 1.6 Hz, 1H, H_c), 3.69 (ddd, ²J(PH) = 19.6 Hz, ³J(H_aH_b) = 12.2 Hz, ³J(H_aH_c) = 9.6 Hz, 1H, H_a), 1.95 (s, 18H, η⁶-C₆Me₆). ¹³C{¹H} NMR (125.71 MHz, CDCl₃): δ 204.94 (d, ²J(PC) = 1.8 Hz, C₂), 134.72 (d, ⁴J(PC) = 2.6 Hz, C_p DPVP), 134.13 (d, ⁴J(PC) = 2.8 Hz, C_p DPVP), 132.66 (d, ²J(PC) = 11.8 Hz, C_o DPVP), 130.86 (d, ³J(PC) = 10.2 Hz, C_m DPVP), 130.56 (d, ³J(PC) = 11.7 Hz, C_m DPVP), 129.15 (d, ²J(PC) = 12.6 Hz, C_o DPVP), 128.96 (s, C_o Ph), 128.71 (s, C_o Ph), 128.71 (s, C_m Ph), 128.64 (s, C_p Ph), 128.45 (s, C_m Ph), 128.42 (s, C_p Ph), 128.32 (s, C_i Ph), 127.78 (s, C_i Ph), 125.57 (d, ¹J(PC) = 64.1 Hz, C_i DPVP), 121.43 (d, ¹J(PC) = 68.5 Hz, C_i DPVP), 111.70 (d, ³J(PC) = 20.4 Hz, C₃), 108.92 (s, η⁶-C₆Me₆), 89.92 (s, C₁), 66.58 (s, C_β), 28.35 (d, ¹J(PC) = 88.1 Hz, C_o), 15.46 (s, η⁶-C₆Me₆). ³¹P{¹H} NMR (202.33 MHz, CDCl₃): δ 36.58 (s, DPVP), -145.01 (sept, ¹J(PF) = 712.7 Hz, PF₆).

Reactions with 1,1-Dimethylpropargylamine, HC≡CC(CH₃)₂NH₂. Method A. To a solution of 0.380 g (0.544 mmol) of **2a** in 18 mL (1:1, v/v) of MeOH/CH₂Cl₂ was added 0.4 mL (3.8 mmol) of HC≡CC(CH₃)₂NH₂. The solution gradually changed color from orange to a deep red-black over the 30.5 h

reaction time. The solvents were removed in vacuo, giving an oily red material and a white solid. The red material was dissolved in MeOH/CH₂Cl₂, and this solution was filtered to remove the white solid; Et₂O was added to the filtrate to crystallize the product(s). (The white solid was not characterized.) Repeated crystallizations gave brown to black oils from which a small amount of the cyclic carbene complex **7** was isolated. The ¹H NMR spectra consistently evidenced the presence of starting material (**2a**) in varying amounts. This prompted us to try the next two methods to increase the amount of **2a** that reacted.

Method B. Dimethylpropargylamine (0.06 mL, 0.51 mmol) was passed through a filter pipet containing Na₂CO₃ (to remove H₂O) directly into a solution of 0.251 g (0.460 mmol) of **1a** in 15 mL of CH₂Cl₂. To this solution was added 0.076 g (0.453 mmol) of NaPF₆ and 5 mL of CH₂Cl₂. When they were heated to reflux, all components were taken into solution, and the red color darkened. The mixture was refluxed for 42.5 h, and then the solvents were removed in vacuo to give a brown oil that was dissolved in CH₂Cl₂ and filtered (nothing was visually removed). The solvent volume was reduced to 2 mL in vacuo, and Et₂O was added to precipitate an orange powder (identified by ¹H NMR spectroscopy to be **1a**) and a brown oil. Repeated precipitations gave 0.047 g of recovered **1a** (18.7%). Continued crystallizations gave a small amount of yellow crystalline **7** and a small amount of red-brown crystalline **8**, as evidenced by ¹H NMR spectroscopy.

Method C. To an orange suspension of 0.296 g (0.541 mmol) of **1a** in 40 mL of 1,2-dichloroethane was added 0.24 mL (2.3 mmol) of HC≡CC(CH₃)₂NH₂ and 0.100 g (0.595 mmol) of NaPF₆. Again, all components were taken into solution upon heating to reflux, and the color of the mixture changed from orange to red to brown. The reaction was monitored by ¹H NMR spectroscopy, which showed the continued presence of **1a**, **7**, and **8** after 56 h of reflux. At this time, 15 mL of absolute EtOH was added in an attempt to make the reaction medium more polar. The mixture was refluxed for another 14 h, at which time the ¹H NMR spectrum of an aliquot showed the same ratios of **1a**, **7**, and **8** as before. The reaction mixture was cooled to room temperature and subjected to column chromatography (2 × 5 cm²) on silica (200–400 mesh, Natland Int. Corp.) with eluting solvents CH₂Cl₂, acetone, and MeOH, sequentially. ¹H NMR spectroscopy showed that the eluted products contained **1a** (CH₂Cl₂), **1a** and **7** (CH₂Cl₂ and 1:1 CH₂Cl₂/acetone), and **1a** and **8** (acetone). Crystallizations of these fractions from CH₂Cl₂/hexane and acetone/Et₂O gave **1a**, **7**, and 0.02 g (0.03 mmol) of mostly pure **8** as yellow-orange crystals from which NMR spectral data were obtained.

Neither **7** nor **8** were obtained pure enough, in large enough quantities, to allow for elemental analyses. All NMR spectroscopic data showed traces to large amounts of starting materials and generally mixtures of **7** and **8**.

[(η⁶-C₆Me₆)Cl(DPVP)Ru=CCH₂CMe₂NH)]PF₆ (7**).** ¹H NMR (499.84 MHz, CDCl₃): δ 7.71–7.67 (m, 4H, H_o Ph), 7.54–7.44 (m, 6H, H_{m,p} Ph), 6.66 (ddd, ²J(PH) = 24.5 Hz, ³J(H_aH_b) = 18.5 Hz, ³J(H_aH_c) = 12.7 Hz, 1H, H_a), 6.30 (ddd, ³J(PH) = 41.5 Hz, ³J(H_aH_c) = 12.7 Hz, ²J(H_bH_c) = 1.5 Hz, 1H, H_c), 6.24 (ddd, ³J(PH) = 22.0 Hz, ³J(H_aH_b) = 18.5 Hz, ³J(H_bH_c) = 1.5 Hz, 1H, H_b), 2.22 (s, 18H, η⁶-C₆Me₆), 1.76 (s, 6H, CMe₂), 1.25 (s, 2H, CH₂), 1.42 (s, 1H, NH). ¹³C{¹H} NMR (125.71 MHz, CDCl₃): δ 134.77 (s, C_β), 132.15 (d, ¹J(PC) = 105.1 Hz, C_i), 131.89 (d, ⁴J(PC) = 2.4 Hz, C_p), 131.31 (d, ²J(PC) = 9.9 Hz, C_o), 131.03 (d, ¹J(PC) = 98.2 Hz, C_o), 128.55 (d, ³J(PC) = 11.9 Hz, C_m), 96.11 (d, ¹J(PC) = 3.3 Hz, η⁶-C₆Me₆), 31.51 (s, CMe₂), 29.62 (s, CH₂), 16.75 (s, η⁶-C₆Me₆), 15.11 (s, CMe₂). ³¹P{¹H} NMR (202.33 MHz, CDCl₃): δ 23.68 (s, DPVP), –144.72 (sept, ¹J(PF) = 712.6 Hz, PF₆).

[(η⁶-C₆Me₆)ClRuCH=C(DPVP)CMe₂NH₂)]PF₆ (8**).** Mp: 198 °C dec. ¹H NMR (499.84 MHz, acetone-*d*₆): δ 9.73 (d, ³J(PH) = 24.0 Hz, CH), 8.08–7.67 (m, 10H, Ph), 7.31 (ddd, ²J(PH) =

24.0 Hz, ³J(H_aH_b) = 18.0 Hz, ³J(H_aH_c) = 12.5 Hz, 1H, H_a), 6.90 (dd, ³J(PH) = 46.5 Hz, ³J(H_aH_c) = 12.5 Hz, 1H, H_c), 6.29 (dd, ³J(PH) = 23.0 Hz, ³J(H_aH_b) = 18.0 Hz, 1H, H_b), 4.84 (dd, ⁴J(PH) = 4.5 Hz, ²J(HH) = 10.5 Hz, 1H, NH₂), 4.19 (d, ²J(HH) = 10.5 Hz, 1H, NH₂), 2.06 (s, 18H, η⁶-C₆Me₆), 1.33 (s, 6H, CMe₂). ¹³C{¹H} NMR (125.71 MHz, acetone-*d*₆): δ 217.74 (d, ²J(PC) = 7.0 Hz, Ru–C), 143.34 (s, C_β), 135.59 (d, ⁴J(PC) = 2.9 Hz, C_p), 135.48 (d, ⁴J(PC) = 2.9 Hz, C_p), 135.27 (d, ²J(PC) = 9.7 Hz, C_o), 135.12 (d, ²J(PC) = 10.4 Hz, C_o), 130.94 (d, ³J(PC) = 12.7 Hz, C_m), 130.84 (d, ³J(PC) = 12.8 Hz, C_m), 121.77 (d, ¹J(PC) = 77.1 Hz, C_o), 121.76 (d, ¹J(PC) = 111.0 Hz, C_i), 121.12 (d, ¹J(PC) = 86.4 Hz, C_i), 95.43 (s, η⁶-C₆Me₆), 68.68 (d, ²J(PC) = 30.2 Hz, CMe₂), 30.95 (s, CMe₂), 16.06 (s, η⁶-C₆Me₆). ³¹P{¹H} NMR (202.33 MHz, acetone-*d*₆): δ 7.10 (s, DPVP), –145.00 (sept, ¹J(PF) = 706.6 Hz, PF₆).

Reaction of 2a and HC≡CC(OH)Ph₂ in the Absence of MeOH. To an orange solution of **2a** (0.319 g, 0.457 mmol) in 10 mL of CH₂Cl₂ was added 0.1 g (0.480 mmol) of HC≡CC(OH)Ph₂. The color changed from orange to purple within minutes. After 4.5 h the solvents were removed in vacuo to yield a purple-red oil. Attempted crystallizations from CH₂Cl₂ and Et₂O gave a small amount of crystalline [(η⁶-C₆Me₆)₂-Ru₂Cl₃]PF₆ (which was identified by an X-ray crystallographic unit cell determination and ¹H NMR spectroscopy⁴) and decomposition of the remainder of the material present.

Reaction of 2a and HC≡CPh in the Absence of MeOH. A solution of 0.307 g (0.440 mmol) of **2a** in 10 mL of CH₂Cl₂ was stirred with 0.05 mL (0.455 mmol) of HC≡CPh for 21 days, by which time the CH₂Cl₂ had evaporated. The orange oil was dissolved in a minimum volume of CH₂Cl₂, washed with hexane, and crystallized from CH₂Cl₂/Et₂O. The carbonyl complex [(η⁶-C₆Me₆)Cl(DPVP)Ru(CO)]PF₆ (**9**) was thus obtained in 11.4% yield (0.034 g) as yellow crystals from an otherwise decomposition-laden mixture.

Complex **9** was also obtained by bubbling CO(g) through an acetone solution (20 mL) of **2a** (0.222 g, 0.319 mmol) for 4 h, followed by removal of solvents in vacuo. Yield: 0.190 g (86.9%). Mp: 192–201 °C. Anal. Calcd for C₂₇H₃₁ClF₆OP₂Ru: C, 47.41; H, 4.57; Cl, 5.19. Found: C, 47.29; H, 4.36; Cl, 5.02. IR (cm^{−1}; CH₂Cl₂): 2014 sh, st ν(CO). IR (cm^{−1}; Nujol): 814, 557 st ν(PF). ¹H NMR (499.84 MHz, CDCl₃): δ 7.47–7.63 (m, 10H, Ph), 6.71 (ddd, ²J(PH) = 25.2 Hz, ³J(H_aH_b) = 17.9 Hz, ³J(H_aH_c) = 12.0 Hz, 1H, H_a), 6.14 (dd, ³J(PH) = 42.5 Hz, ³J(H_aH_c) = 12.0 Hz, 1H, H_c), 5.41 (dd, ³J(PH) = 21.5 Hz, ³J(H_aH_b) = 17.9 Hz, 1H, H_b), 2.00 (s, 18H, η⁶-C₆Me₆). ¹³C{¹H} NMR (125.70 MHz, CDCl₃): δ 196.49 (d, ²J(PC) = 24.9 Hz, Ru–CO), 133.72 (d, ²J(PC) = 9.9 Hz, C_o), 133.34 (d, ²J(PC) = 9.9 Hz, C_o), 132.65 (d, ⁴J(PC) = 2.4 Hz, C_p), 132.56 (s, C_β), 132.23 (d, ⁴J(PC) = 2.8 Hz, C_p), 130.16 (d, ¹J(PC) = 53.0 Hz, C_o), 129.38 (d, ³J(PC) = 10.8 Hz, C_m), 129.07 (d, ³J(PC) = 10.8 Hz, C_m), 126.18 (d, ¹J(PC) = 55.6 Hz, C_i), 126.77 (d, ¹J(PC) = 54.9 Hz, C_i), 113.57 (d, ¹J(PC) = 1.9 Hz, η⁶-C₆Me₆), 16.20 (s, η⁶-C₆Me₆). ³¹P{¹H} NMR (202.33 MHz, CDCl₃): δ 34.41 (s, DPVP), –145.00 (sept, ¹J(PF) = 712.4 Hz, PF₆).

Catalysis. Phenylacetylene (2 mL, 18 mmol) was added to a suspension of **1a** (0.250 g, 0.457 mmol) in 10 mL of 95% EtOH. Upon heating, all components were taken into solution, and the color darkened. After a 17 h reflux, the solution was cooled to room temperature and the solvents were removed in vacuo to give a red oil. The oil was washed several times with hexane, and the yellow washings were passed through a flash column packed with Celite and silica, with most of the red inorganic material being left on the Celite. The inorganic fraction was then washed from the column with CH₂Cl₂ and MeOH. Solvent removal and vacuum distillation (0.27 mmHg, 78 °C) of the organic fraction yielded 1.534 g of a pale yellow viscous liquid. ¹H NMR and FT-IR spectroscopy and GC/MS have identified the products as acetophenone, hexamethylbenzene, and an unknown compound in a ratio of 81.4:15.7:2.9. The red inorganic fraction has not been fully characterized as yet.

Table 10. Crystallographic Data

	1b	1c	3a	3b	3c	4a
empirical formula	C ₁₅ H ₂₇ Cl ₂ PRu	C ₃₀ H ₃₃ Cl ₂ PRu	C ₂₉ H ₃₇ ClF ₆ ·OP ₂ Ru	C ₁₈ H ₃₃ ClF ₆ ·OP ₂ Ru·C ₃ H ₆ O	C ₃₃ H ₃₉ ClF ₆ ·OP ₂ Ru·C ₄ O	C ₃₅ H ₄₁ ClF ₆ ·OP ₂ Ru·C _{1.50} H ₃ O _{0.50}
fw	410.31	596.50	714.05	635.98	828.14	819.18
cryst syst	orthorhombic	triclinic	orthorhombic	monoclinic	monoclinic	monoclinic
space group	<i>Pbca</i>	<i>P</i> $\bar{1}$	<i>P</i> 2 ₁ 2 ₁ 2 ₁	<i>P</i> 2 ₁ / <i>n</i>	<i>P</i> 2 ₁ / <i>c</i>	<i>C</i> 2/ <i>c</i>
<i>a</i> (Å)	15.2968(14)	8.9314(11)	8.3402(8)	17.385(6)	14.840(2)	24.2254(13)
<i>b</i> (Å)	17.8266(10)	9.0629(9)	13.7264(12)	8.9043(15)	8.616(3)	10.6895(14)
<i>c</i> (Å)	26.3270(17)	17.8273(17)	27.022(3)	18.548(3)	29.172(4)	29.163(2)
α (deg)	90	89.243(8)	90	90	90	90
β (deg)	90	89.432(11)	90	91.92(2)	94.846(5)	104.479(6)
γ (deg)	90	65.522(8)	90	90	90	90
<i>V</i> (Å ³)	7179.1(9)	1313.2(2)	3093.5(5)	2869.6(13)	3716.7(14)	7312.0(12)
<i>Z</i>	16	2	4	4	4	8
<i>d</i> _{calcd} (g/cm ³)	1.518	1.509	1.533	1.472	1.480	1.488
μ (mm ⁻¹)	1.247	0.879	0.755	0.805	0.642	0.650
R1(<i>F</i>)/wR2(<i>F</i> ²) ^a	0.0772/0.0734	0.0521/0.1051	0.0819/0.1391	0.0808/0.1977	0.0748/0.1797	0.0636/0.1734

	4b	4c	5	6	8	9
empirical formula	C ₂₄ H ₃₇ ClF ₆ ·OP ₂ Ru	C ₃₉ H ₄₃ ClF ₆ ·OP ₂ Ru·CH ₂ Cl ₂	C ₃₀ H ₃₇ ClF ₆ ·OP ₂ Ru	C ₄₁ H ₄₁ ClF ₆ P ₂ Ru	C ₃₁ H ₄₁ ClF ₆ ·NP ₂ Ru	C ₂₇ H ₃₁ ClF ₆ ·OP ₂ Ru
fw	654.00	925.12	726.06	846.20	740.11	683.98
cryst syst	orthorhombic	triclinic	monoclinic	monoclinic	triclinic	monoclinic
space group	<i>Pbca</i>	<i>P</i> $\bar{1}$	<i>P</i> 2 ₁ / <i>c</i>	<i>P</i> 2 ₁ / <i>n</i>	<i>P</i> $\bar{1}$	<i>P</i> 2 ₁ / <i>c</i>
<i>a</i> (Å)	13.3348(17)	9.243(3)	13.8695(7)	10.3675(8)	9.8514(17)	10.7954(9)
<i>b</i> (Å)	15.537(4)	10.934(4)	8.3371(6)	23.5252(12)	11.0147(13)	15.450(2)
<i>c</i> (Å)	27.037(3)	20.766(5)	26.956(2)	16.4003(15)	16.392(2)	17.280(2)
α (deg)	90	78.132(18)	90	90	77.717(8)	90
β (deg)	90	83.389(18)	96.906(6)	101.269(7)	76.579(11)	91.623(7)
γ (deg)	90	89.359(19)	90	90	87.082(11)	90
<i>V</i> (Å ³)	5601.6(17)	2039.9(10)	3094.4(4)	3922.9(5)	1690.6(4)	2881.0(6)
<i>Z</i>	8	2	4	4	2	4
<i>d</i> _{calcd} (g/cm ³)	1.551	1.506	1.559	1.433	1.454	1.577
μ (mm ⁻¹)	0.825	0.718	0.756	0.606	0.692	0.807
R1(<i>F</i>)/wR2(<i>F</i> ²) ^a	0.0910/0.1519	0.0830/0.1393	0.0628/0.1083	0.0678/0.1580	0.0883/0.2225	0.0692/0.1449

^a Final *R* indices have $I > 2\sigma(I)$. $R1(F) = \sum(|F_o| - |F_c|)/\sum(|F_o|)$; $wR2(F^2) = [\sum w(|F_o|^2 - |F_c|^2)|^2/\sum w(|F_o|^2)]^{1/2}$.

X-ray Crystallographic Studies. Single crystals of **1b**, **3a–c**, **4a–c**, **5**, **6**, **8**, and **9** suitable for X-ray diffraction were obtained as follows: slow diffusion of Et₂O into a CHCl₃ solution of complex **1c**, slow diffusion of hexane into a benzene solution of complex **1b**, slow diffusion of Et₂O into CH₂Cl₂ solutions of complexes **3a**, **4a**, **b**, and **9**, slow diffusion of Et₂O into a CHCl₃/acetone solution of complex **3b**, and slow diffusion of Et₂O into acetone solutions of complexes **4c**, **5**, **6**, and **8**. The crystals were mounted on glass fibers, coated with epoxy, and placed on a Siemens P4 diffractometer. Intensity data were collected in the ω mode with graphite monochromated Mo K α radiation ($\lambda = 0.71073$ Å). Three check reflections, monitored every 100 reflections, showed random (<2%) variation during the data collections. The data were corrected for Lorentz, polarization effects, and absorption (using an empirical model derived from azimuthal data collections). Scattering factors and corrections for anomalous dispersion were taken from a standard source.²⁶ Calculations were performed within the Siemens SHELXTL Plus (version 5.10) software package on a PC. The structures were solved by direct methods (**1b**, **3a**, and **9**) or by Patterson methods (**1c**, **3b**, **c**, **4a–c**, **6**, and **8**).

Anisotropic thermal parameters were assigned to all non-hydrogen atoms. Hydrogen atoms were refined at calculated positions with a riding model in which the C–H vector was fixed at 0.96 Å. Hydrogen atoms were not added to the solvent Et₂O molecule in the structure solution of **3c**. There is half of an acetone molecule in the unit cell of **4a**. The data were refined by the method of full-matrix least squares on *F*². Final cycles of refinement converged to the R1(*F*) and wR2(*F*²) values given in Table 10, where $w^{-1} = \sigma^2(F) + 0.001F^2$.

Acknowledgment. An award from the Research Corp., for which we are grateful, supported this research. We thank Johnson Matthey Aesar/Alfa for a generous loan of RuCl₃·H₂O and the National Science Foundation (Grant No. CHE-9214294) for funds to purchase the 500 MHz NMR spectrometer.

Supporting Information Available: Listings of atom coordinates, bond distances and angles, thermal parameters, anisotropic refinements, and hydrogen atom coordinates for **1b**, **3a–c**, **4a–c**, **5**, **6**, **8**, and **9**. This material is available free of charge via the Internet at <http://pubs.acs.org>.

(26) *International Tables for X-Ray Crystallography*, D. Reidel: Boston, MA, 1992; Vol. C.